Journal of Applied Physics REVIEW pubs.aip.org/aip/jap

Review of radiation-induced defects in GaAs

Cite as: J. Appl. Phys. 138, 070701 (2025); doi: 10.1063/5.0279267
Submitted: 6 May 2025 · Accepted: 27 July 2025 ·
Published Online: 18 August 2025

X.-Y. Liu,[a] C. N. Singh, E. R. Kennedy, S. Huang, S. P. Fluckey, C. Matthews, and B. P. Uberuaga

AFFILIATIONS

Los Alamos National Laboratory, Los Alamos, New Mexico 87545, USA

[a]Author to whom correspondence should be addressed: xyliu@lanl.gov

ABSTRACT

Radiation-resilient optoelectronic materials are highly desired in space and nuclear applications, and understanding the relevant defects and electronic processes in those materials is crucial for both current and next-generation applications. GaAs is a prototypical semiconductor that serves as a foundational system for describing and understanding optoelectronic devices. In this review, both experimental studies and molecular dynamics (MD) simulations of irradiated GaAs are reviewed, with particular emphasis on the deep-level transient spectroscopy, irradiation-induced amorphization zones, and MD predictions of damage structures. The MD results are also compared to predictions of the non-ionized energy-loss model. Recent theoretical studies, in particular, density functional theory based calculations on the simple intrinsic defects and defect clusters in GaAs, are also reviewed. These defects have an important role in dictating the evolution of GaAs in radiation damage environments, as they impact the coupled dynamics of charge carriers. Finally, possible gaps and challenges toward the general understanding of defect evolution in GaAs are discussed.

I. INTRODUCTION

GaAs is the base material for many optoelectronics devices. Since the early work of Hall *et al.* demonstrating coherent light emission from GaAs junctions,[1] this material has gained popularity in research and development centering around optoelectronics applications. In many situations, such as in space and nuclear applications, the deployed optoelectronic devices are exposed to harsh radiation environments. In these conditions, various defects can form, which greatly influences the device performance. This interaction of energetic particles with matter gives rise to materials that, at times, have totally unique properties. Thus, understanding radiation-induced defects and defect complexes is becoming increasingly important in GaAs and has the potential to drive innovation in critical technologies like solar cells, lasers, and thermoelectric generators.

One of the earliest experimental studies of defects in GaAs is the work of Williams in 1966.[2] Although the defect studied there is associated with oxygen impurities rather than intrinsic defects, this work nevertheless opened the experimental avenue of studying the deep centers (electronic states deep in the bandgap of the material induced by defects) in GaAs using capacitance techniques.[2] This technique was later developed to a more advanced and powerful tool known as deep-level transient spectroscopy (DLTS) to probe the energy levels of defects in III–V semiconductors including GaAs.[3,4] There have been numerous studies on radiation-induced defects in GaAs since then. Arguably, the last comprehensive review on defects in GaAs, by Bourgoin *et al.*,[5] was almost 30 years ago. Since that review, there has been enormous advancement in the fundamental understanding of defects in GaAs from both a modeling and experimental perspective, but a modern review summarizing all this information is missing from the literature. This review serves to capture that work and provide clarity on the outstanding problems in the field.

The arrangement of this review is as follows: To start, we first review radiation effects in GaAs in general. This is followed by the review of studies on different defects: point defects and defect complexes induced by irradiation, defect clusters, and charge dynamics. We then highlight the current gaps and challenges toward a comprehensive understanding of defect evolution in radiation environments and the possible impact of radiation-induced defects on the electronic behavior of GaAs. Finally, a summary is given.

II. FUNDAMENTALS: PROPERTIES OF GaAs AND DEFECTS IN SEMICONDUCTORS

A. Properties of GaAs

GaAs was first described by Goldschmidt in 1929.[6] However, it was not until 1952 that Welker described the electronic

properties of the compound,[7] which initiated worldwide interest in the material for semiconductor devices. Since then, GaAs has been used in transistors of various types, solar cells, laser diodes,[1] and spintronics.[8]

As highlighted in Fig. 1(a), GaAs is a cubic material with the zinc blende (or cubic sphalerite) structure, space group F-43m, and a lattice constant of 0.565 nm. Ga and As each reside on their own fcc sublattice; thus, the GaAs structure can be conceptualized as two interpenetrating fcc lattices that are offset from one another by (¼, ¼, ¼). Each of the atoms is in a tetrahedral environment, surrounded by four neighbors of the opposite type. If all of the atoms were of one type, such as C, the structure becomes identical to that of diamond. GaAs can adopt other structures, particularly at high pressures,[10] but this structure is the most common and is the structure GaAs adopts in devices.

GaAs is a direct bandgap material with a bandgap of 1.42 eV (at room temperature)—the band structure is shown in Fig. 1(b). As a direct bandgap material, electron excitations require only energy, not momentum, making GaAs amenable for optical devices (in contrast to Si, which has an indirect bandgap). Compared to Si, GaAs has a higher electron mobility. GaAs is also a semi-insulating compound.[11] In conductive semiconductors, electrically active impurities can easily introduce states near the valence or conduction band (CB) edges, thereby enhancing carrier concentrations (more on this later). In contrast, impurities in semi-insulators tend to pin the Fermi level near midgap, which strongly suppresses free-carrier concentrations and results in much higher resistivity. GaAs is unique in that it can be prepared either as a high-resistivity semi-insulator or as a p- or n-type semiconductor. This affords it great flexibility as the foundation of semiconductor devices.

Finally, it is important to note that Ga and As come from different groups in the periodic table. In conventional notation, Ga is a group III and As is a group V element. (Note that this nomenclature is somewhat outdated—in the newer international naming convention for the periodic table, these are now called groups 13 and 15, losing their connection to valence. Thus, in the semiconductor literature, these are often still referred to their old group classification.) This can also be interpreted as their valence: Ga has three valence electrons while As has five. This is important for understanding the defect chemistry in this compound.

B. Defects in semiconductors

Defects are unavoidable in materials but in many cases, they are the source of functionality. In semiconductors, defects are typically separated into two classes: dopants (and impurities) and point defects. Classifying dopants as defects may seem counterintuitive as they are intentionally added to the semiconductor to change the properties of the material. However, from a fundamental perspective, their impact is often similar in nature to other point defects, so we will consider them as such in this treatment.

Two types of dopants are usually added to semiconductors: p- and n-type dopants. Both have a different number of valence electrons compared to the host site upon which they sit, and, in a compound semiconductor such as GaAs, the same dopant can be either n- or p-type depending on where it sits [see Fig. 2(a)]. Typically, a p-type dopant has a lower electronic valence than the host site. As such, it tends to attract, or accept, an electron from the matrix atoms. The capture of an electron effectively emits a hole into the matrix. In contrast, an n-type dopant has more electrons than the host atom and, thus, emits, or donates, an electron to the matrix. Thus, p-type dopants are referred to as acceptors and n-type dopants are donors.

GaAs is a so-called III–V semiconductor; as noted earlier, this means that it is a compound of atoms that nominally have three (Ga) or five (As) valence electrons. Thus, to achieve n-type doping, either host atom must be replaced by an atom with a larger number of valence electrons: more than five for As and more than three for Ga. Typical dopants in GaAs are highlighted in Fig. 3. In GaAs, n-type dopants include Te and S when they are substituted for As and Sn, Si, and Ge when they are substituted for Ga. On the other hand, p-type doping involves replacing Ga or As with lower valence species, two for Ga or four for As. Typical p-type dopants include Be, Zn, or Cr when substituted for Ga, and Si, Ge, or C when substituted for As. Note that dopants with four valence electrons, such as Si and Ge, can be either p- or n-type depending on where they sit in the lattice—these are often called amphoteric dopants.

Dopants are used to engineer the properties of semiconductors by introducing electronic states in the gap that are either filled with electrons (n-type) or holes (p-type). As shown in Fig. 2(b), this shifts the Fermi level and changes the concentration and mobility of free electrons or holes.

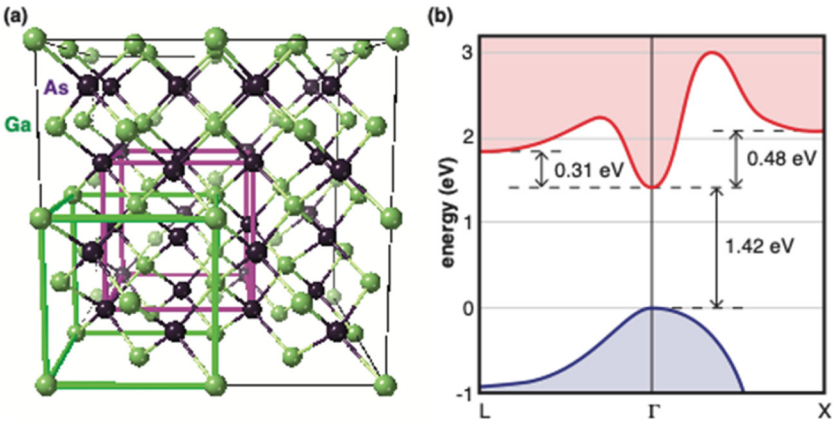

FIG. 1. (a) The structure of GaAs. The elemental fcc structure of the Ga and As sublattices is highlighted by the green and purple cubes, respectively. (b) The elementary band structure of GaAs, highlighting the direct bandgap and a few other prominent features within the band structure. The conduction band is highlighted in red while the valence band is highlighted in blue. Adapted from L. Q. Tian and W. Shi, J. Appl. Phys. **103**, 124512 (2008). Copyright 2008 AIP Publishing LLC.[9]

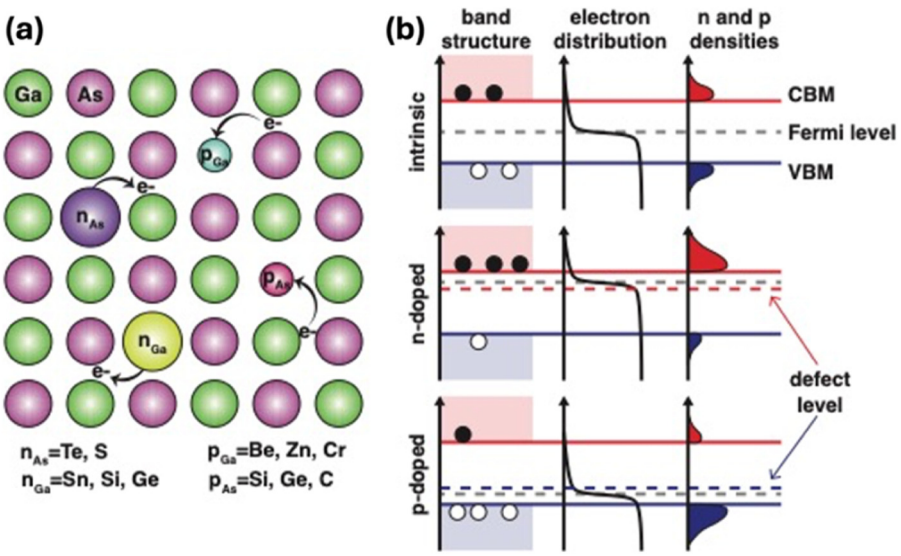

FIG. 2. (a) Schematic showing the type of dopants that are common in GaAs. (b) Schematic of how doping changes the band structure and shifts the population of holes and electrons in the material. Adapted from S. M. Sze and K. K. Ng, *Physics of Semiconductor Devices* (John Wiley & Sons, 2006). Copyright 2006 John Wiley & Sons.[12]

Point defects have a similar impact on the electronic structure, but in contrast to dopants, these often occur unintentionally and uncontrollably. Just like dopants, defects can also donate or accept carriers from the host atoms, altering the carrier population.[13,14] In a compound semiconductor, the point defects are interstitials, vacancies, and antisites. The interstitials and vacancies not only impact the electronic properties of the material but also control atomic diffusion within the material. As the name implies, vacancies are the atomic analog of holes, i.e., missing atoms in the crystal structure of the material. In contrast, interstitials are excess atoms in the atomic structure, filling the space between the lattice sites of the structure.

In addition to where a defect sits in the lattice, there is an additional degree of freedom for any point defect—its charge state.

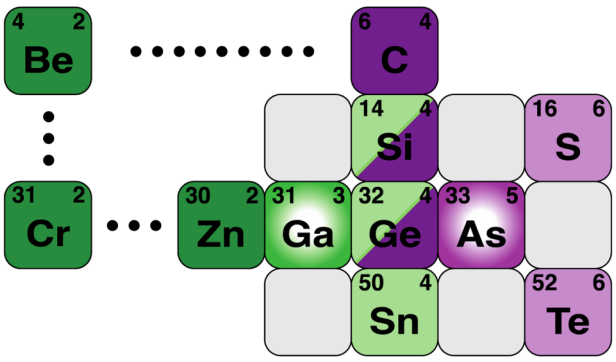

FIG. 3. A section of the periodic table showing common dopants in GaAs, highlighting the valence state as relevant for GaAs doping. Dark green (purple) elements are p-type dopants when substituted for Ga (As), while light green (purple) elements are n-type dopants for Ga (As). Note that dopants like Si and Ge can act as either p- or n-type depending on which host element they replace.

In the absence of any transfer of electrons, a Ga interstitial—typically notated as Ga_i—would be neutral, but it can capture or emit electrons, changing its charge state. The various energies at which these transitions occur lead to a multitude of different states in the gap and also define how likely these transitions are to occur. Charge states are denoted by explicitly labeling the defect with the net charge: Ga_i^0 for a neutral Ga interstitial, Ga_i^{-1} for an interstitial that has captured one electron, and Ga_i^{+1} when it has captured a hole (or emitted one electron). Similar notation is used for As interstitials (denoted as As_i) and vacancies on either sublattice (V_{Ga} or V_{As}). In reality, these defects can carry a range of charge states, complicating both their understanding and their impact on properties. This will be discussed in more depth later.

While interstitials and vacancies are present in all solids, including elemental solids, antisites are only present in compound materials. Antisites are atoms in the GaAs crystal structure that occupy a site that a different element would normally occupy, that is, a Ga on an As site or an As on a Ga site. These are denoted as Ga_{As} and As_{Ga}. Since Ga and As have different valence states, creating antisites on either sublattice naturally creates an electrically active "dopant." Ga_{As} has the possibility of capturing up to two electrons to achieve the same valence state as As and, correspondingly, As_{Ga} can capture up to two holes. Thus, these two defect states may exhibit a −2 and +2 charge state, respectively, though other charge states are certainly possible and maybe even likely. Thus, as we create defects of any type in the compound, new states will be created in the bandgap and, depending on the concentration of those defects, these can act as isolated traps for electrons and holes or even create new bands that can impact various properties of the material.

III. RELEVANCE OF RADIATION DAMAGE TO GaAs DEVICE PERFORMANCE

Radiation-resilient optoelectronic materials are highly desired in space and nuclear applications,[15,16] and understanding the

defects with the greatest impact on optical and electronic processes in GaAs is crucial for both predicting performance and designing new devices for current and next-generation applications.[17] The relevant GaAs-based devices include a range of optoelectronic devices, including intersatellite optical links, light-emitting diodes (LEDs), laser diodes, GaAs-based metal semiconductor field effect transistors (FETs) and logic gates, near-infrared imaging devices, and solar cells. These devices could all be exposed to different types and fluences of radiation as part of their normal operation.[18]

The overall radiation resistance of many technologically significant optoelectronic devices is governed by radiation-induced defects and defect-mediated carrier decay rates.[19,20] Two notable examples that illustrate this concept are GaAs-based laser diodes and solar cells. The efficiency of laser diodes is controlled by the rate of electron–hole pairs decaying into emitted photons,[21] while the efficiency of solar cells is controlled by the rate of photons turned into dissociable electron–hole pairs.[22] Radiation-induced point defects greatly impact these decay pathways by promoting thermal relaxation/decay at the expense of optically active pathways.[15,23] In solar cells, this results in electron–hole pairs recombining, thermally, faster than they can be extracted as useful current.[24] In laser diodes, this amounts to injected electron–hole pairs recombining to generate heat rather than light.[21] Because these and other optoelectronic devices are often deployed in the harsh radiation environments of space and nuclear systems, significant effort has been devoted to understanding the complex relation between radiation-induced point defects and overall device performance. Being able to predict the performance of these systems before they are deployed is a technical challenge because it requires bridging vast length and time scales.

IV. GENERAL OVERVIEW OF RADIATION EFFECT IN GaAs

Depending on the irradiation spectrum—γ-rays, electrons, neutrons, protons, ions—the radiation damage in GaAs is different. For example, while γ-rays typically induce relatively short-lived ionization damage, electron radiation mostly produces clearly separated and stable point defects in GaAs.[5] Due to this behavior, early studies have made extensive use of electron irradiation to develop the foundational understanding of point defect and defect complex behavior in GaAs. Neutrons, protons, and heavier ions can cause dense cascades of permanently displaced atoms, giving rise to more complicated structures than either γ-ray or electron irradiation. In this section, we will first review the experimental observation of radiation effects in GaAs. This is followed by molecular dynamics (MD) simulation results of cascade damage in GaAs, which reveal the structural details in irradiated GaAs. Finally, the nonionizing energy-loss (NIEL) model[25] in GaAs, which is commonly used to describe damage levels in semiconductors, is compared with MD predictions.

A. Experimental observation of radiation effects in GaAs

While heavy ion irradiation and high dose conditions can produce large-scale damage to GaAs lattice, many forms of irradiation result in point defects and local electronic structure reconfigurations that are difficult to detect with traditional bulk characterization methods. Early experimental studies of irradiated GaAs, particularly for a neutron radiation environment, focused on changes in electrical properties.[26–32] Williams *et al.* studied such changes in n-type GaAs as a result of fast neutron irradiation.[31] The main effect of fast neutron irradiation is the removal of the majority carriers due to the trapping of mobile charge carriers by radiation-induced energy levels created within the bandgap.

As a result of neutron irradiation, the position of the Fermi level in the bandgap shifts away from the conduction band toward midgap as it depends on the free-carrier density. It was found that there is a linear relationship between neutron fluence and the Fermi-level shift that accounts for the observed change in carrier concentrations,[31] which results in a non-linear dependence of carrier concentrations on neutron fluence. A second effect of the irradiation is the degradation of carrier mobility, only evident at low temperatures as a result of carrier scattering by the defect traps.[31]

While many techniques have been applied to the study of optoelectronic properties of semiconductors, there are a few spectroscopic measurements that are routinely applied for defect characterizations. For example, deep-level transient spectroscopy (DLTS) is often used to characterize defect energy levels within the bandgap of irradiated GaAs and other semiconductors. DLTS was developed by Lang *et al.*[3,33–35] and it is a powerful tool to characterize the deep-level defects in GaAs. It is based on a junction-capacitance technique[2,36,37] and can measure the activation energy for thermal emission of a carrier from a trap state to the nearby band edges. It can also probe the dynamics of charge carriers with the defect trap states within the bandgap,[35,38–41] a subject we will return to in Sec. VII.

One advantage of DLTS over purely electrical measurements (such as resistivity measurement) is that DLTS are highly specific to a particular defect. For example, Martin *et al.*[42] used DLTS to study the carrier dynamics of a midgap donor level, often called the *EL*2 defect. (For electron traps, the DLTS levels are usually labeled with the symbol *E*, such as *E*1-9 or *EL*1-11, while hole traps are labeled with the symbol *H*.[43] Following that convention, we will also use the same classification in this paper.) Similarly, *En* series are used to label broader peaks in DLTS, under thermal annealing in neutron-irradiated GaAs. Figure 4 shows the DLTS spectra recorded on Bridgman-grown GaAs doped with Si, both as irradiated by neutrons and after annealing at various temperatures post-irradiation. The level of DLTS signal corresponds to the defect concentration in the sample. This figure highlights the reduction in *EL*2 defect concentration after annealing and allows for the extraction of the *EL*2 trap energy.

Often, DLTS is combined with techniques such as cathodoluminescence (CL), photoluminescence (PL), UV–Vis spectroscopy, and Hall transport measurements to gain a more comprehensive understanding of the impact of radiation-induced defects on device performance and band structure.[44,45] While CL uses electron beam and PL uses photoexcitation to probe the optical properties, UV–Vis is an absorption spectroscopy. Hall transport measurements provide information about the carrier type (n- or p-type), carrier density, and carrier mobility within the material. A comprehensive analysis involving DLTS, PL, and Hall transport

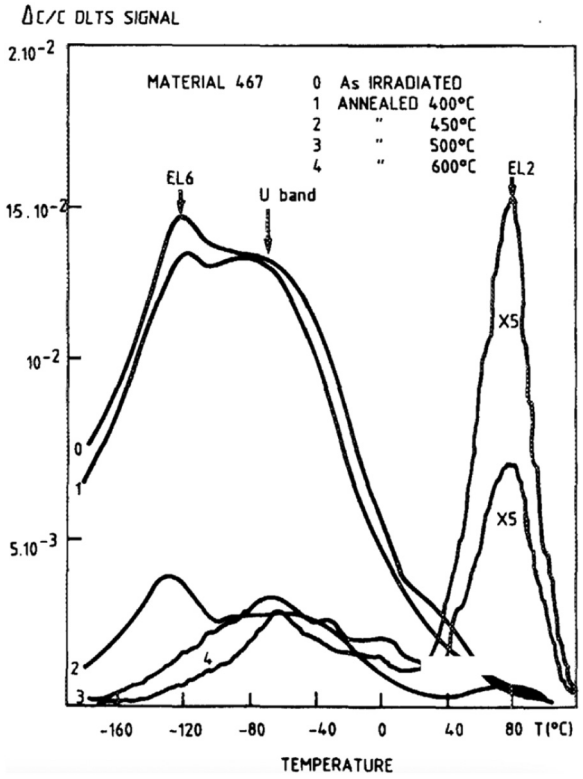

FIG. 4. DLTS spectra recorded on Bridgman-grown GaAs doped with Si ($n = 1.8 \times 10^{17}$ cm^{-3}) as irradiated and after annealing at various temperatures at a fluence of 3.1×10^{15} n/cm^{-2}. Reproduced with permission from G. M. Martin, E. Estève, P. Langlade, and S. Makram-Ebeid, J. Appl. Phys. **56**, 2655–2657 (1984). Copyright 1984 AIP Publishing LLC.[42]

measurements was employed by Pons and Bourgoin, and Swaminathan[46,47] to map out the (primarily electron-induced) point defects in GaAs. The results were summarized in the 1988 review paper by Bourgoin *et al.*[5] Interested readers are encouraged to find out details there. Later developments in both theoretical and experimental understanding of point defects and defect complexes in GaAs due to irradiation will be covered in Sec. V. Another complementary and powerful tool to characterize defects in GaAs is electron paramagnetic resonance (EPR). Two experimental studies stand out, by Worner *et al.*[48] and Goltzene *et al.*[49] Both studies aimed to measure the As_{Ga} antisite defect population in fast neutron-irradiated GaAs. Both studies suggest that there is a nonlinear growth in defect concentration as a function of fast neutron total fluence. The defect population characterized through EPR is also influenced by the as-grown impurity concentration in samples.

Under neutron irradiation, there are several experimental results suggesting more extended defects could be formed that are typically not found in electron irradiated samples. Auret *et al.*[45,50] used DLTS to identify *En*1-5 defect levels in neutron-irradiated n-type GaAs and found broader peaks. These peaks were speculated to be related to the presence of extended defects, but conclusive studies are not available. In GaAs DLTS, the "*U*-band" is a broad, anomalous feature observed in DLTS spectra, particularly after neutron irradiation. Above a critical fluence level, the "*U*-band" was observed by several authors,[44,51,52] suggesting a feature that only appears in more heavily damage GaAs. Warner *et al.*[53] studied GaAs under 227 MeV proton irradiation. The evolution of the *U*-band defect as determined by DLTS seems to occur at active recombination centers, as observed in electron beam induced current (EBIC) measurements, in which the generation of electron–hole pairs under an electron beam informs on carrier mobility and defect characteristics. The charge recombination centers appear to be produced by high-energy recoils creating defect clusters. Defect clusters induced by irradiation in GaAs will be covered in Sec. VI.

The integration of dedicated spectrometers with optical and electron microscopes enables spatially resolved analysis of the optoelectronic properties of GaAs. In recent years, micro-photoluminescence (micro-PL) has been used to measure the bandgap variations across defects in GaAs by analyzing emitted luminescence.[54,55] Notably, micro-PL has been employed to map band-to-band electron emissions and band-to-impurity luminescence around pinhole defects in GaAs, revealing a distinct bimodal luminescence peak structure and a reduced bandgap for antisite impurity transitions compared to the pristine crystal.[56]

Additionally, CL and electron energy-loss spectroscopy (EELS) are commonly used to characterize the band structure at the submicrometer scale. Early studies on ion-irradiated GaAs utilized EELS to observe changes in the band structure and the generation of dangling Ga bonds as a function of depth below the irradiated surface after Ar^+ irradiation.[57] EELS experiments involving low-energy N_2^+ irradiation demonstrated the controllable implantation of nitrogen into GaAs, significantly altering its electronic properties.[58] Given that the damage profile—i.e., the variation in defect concentration and implanted ions as a function of depth—changes with irradiation conditions, the ability to probe these spatially dependent modifications using cross-sectional transmission electron microscopy (TEM) provides valuable experimental insight. TEM enables direct visualization and quantification of depth-resolved structural changes, including dislocation loops, cavities, and phase changes, allowing correlation with ion dose or displacements per atom (dpa).

While much of the literature on irradiated GaAs has concentrated on point defects and amorphous zones, recent studies employing advanced microscopy techniques have provided valuable insights into extended defects. Atomic-resolution TEM and high-angle annular dark-field imaging (HAADF) STEM observations have revealed the formation and evolution of dislocation loops and stacking faults in GaAs under ion irradiation, indicating that these extended defects are indeed present and can be characterized with high spatial resolution.[59,60] Notably, a combination of ion range calculations and MD simulations has shown that the dominant damage mode in GaAs under ion irradiation, including MeV He ions and low-energy self-recoils, is the formation of defect clusters, rather than isolated point defects. Interstitials are found to dominate among the isolated defects, but clustered damage dominates overall.[61]

It is commonly observed that in III–V compounds (and covalently bonded semiconductors more broadly) sufficient irradiation

can lead to amorphization zones/layers. As noted by several authors, GaAs is no exception.[62–65] Irradiation of GaAs with various ion species (B, C, O, Si, Ar, and Ge) at energies around 100 keV has been shown to induce amorphous layer formation under a wide range of conditions. The resulting amorphous layers can reach considerable thicknesses (50–300 nm, depending on the ion), with their extent influenced by factors such as ion mass, substrate temperature, and flux, rather than solely by displacement damage.[64] For proton irradiation at 30 keV, the critical fluence required for amorphization has been reported as 3.6×10^{17} protons/cm^2.[66] Unsurprisingly, Kr irradiation at 1 MeV requires a much lower fluence of 2×10^{14} ions/cm^2 to produce a layer of amorphization.[67] Additionally, the formation of an amorphous zone is shown to be extremely sensitive to implanting temperature.[62] Further, Bench *et al.*[63] found that, upon warming to room temperature, the amorphous zones decreased in size and density as the sample temperature was increased above 200 K. With sufficient time at 300 K, the amorphous zones decreased in size and eventually recrystallized completely, leaving no trace of their prior existence. While gradual recrystallization has been observed at room temperature, the recrystallization temperature of GaAs is cited around 500 K with annealing processes often in the 500–700 K range, depending on sample geometry.[68–70] Proton irradiation of GaAs solar cells has been studied through device modeling and optical techniques like PL and current–voltage (I–V) measurements, revealing functional degradation due to defect-induced damage. These defects reduce minority carrier diffusion length and increase recombination, consistent with simulations.[71] It is unclear if neutron or proton irradiation could produce a similar level of amorphization in GaAs to those observed under ion irradiation conditions or to what extent that amorphization might occur at various operating temperatures.

The dynamics of generation, recovery, and accumulation of ion irradiation damage in GaAs has been a focus of more recent experimental studies.[72–74] Kanayama explored the recovery and accumulation of ion irradiation damage, revealing a dose rate dependence (the higher dose rate led to the heavier damage) in GaAs.[72] Debelle *et al.* studied the effect of energy deposition on the amorphization kinetics in dual-ion beam irradiated GaAs.[74] They found that electronic energy deposition can induce an efficient dynamic annealing of the damage created in collision cascades.

B. Molecular dynamics simulation of radiation damage in GaAs

MD simulation of radiation damage offers atomistic detail of damage structures. MD uses interatomic potentials to simulate the motion of interacting atomic particles in material systems. MD provides direct insight into the defect structure produced during the collision cascade damage event, though timescale limitations hinder the study of the longer-time (e.g., microseconds and beyond) evolution of those defects. Large-scale MD studies of irradiation effects in GaAs began with the work of Nordlund *et al.*[61] Before that, few studies examined the irradiation damage processes and those that did were limited to quite low energies.[75,76] To count the number of defects, a standard Wigner–Seitz (WS) method is used in Nordlund *et al.*'s MD simulations.[61]

Part of the reason that GaAs being less well studied is because of the unreliability of the interatomic potentials used in MD simulations to describe the atomic force interactions in GaAs. In addition, charges and carrier population, which affect defect formation energies, are neglected in the interatomic potentials. Nordlund *et al.*'s work[61] was considered a substantial step in the ability to reliably predict the damage distributions and amorphous zones produced during collision cascades in GaAs. Nordlund and coworkers[61,77–79] found that for Ga and As recoils with energies up to 10 keV, a significant portion of the damage resides in large amorphous clusters or amorphous pockets. In addition, the number of antisites is an order of magnitude smaller than the total number of defects. The authors concluded that, since the amorphous zones anneal out at room temperature and much of the remaining damage is in small clusters which can also be expected to anneal out easily, the antisites will be one of the most important defects remaining at high temperatures.

Björkas *et al.* studied the damage produced by high-energy 100 keV–10 MeV H^+, He, Ne, and Ni ions in GaAs using MD simulations.[78] They found that large amorphous clusters were not formed by H^+ irradiation, while some did form for Ni irradiation. This observation is commensurate with experiments.[80] The authors suggest that for heavy ion irradiation, as compared to light ion irradiation, there is an increasing fraction of damage concentrated in large clusters, which causes a greater change in carrier decay time as observed in experiments.[81]

Later, using the same interatomic potential as Björkas *et al.*,[78] Gao and co-workers carried out primary knock-on atom (PKA) recoil MD simulations for displacement cascades up to 20 keV,[82] however, for a much larger crystal supercell of 1×10^6 atoms employed for their MD simulations. In addition, the short-range interactions for high-energy particles with GaAs were further modified to match the "universal" screening function Ziegler–Biersack–Littmark (ZBL) potential.[83] This potential gives a good representation of high-energy scattering of atoms in solids.

Figure 5 shows the final defect states after (a) 2, (b) 5, and (c) 20 keV cascade in GaAs observed in Gao *et al.*'s simulations.[82] The transition from a single pocket of atomic displacements to multiple subcascades is readily apparent. The defects generated by a PKA energy less than 2 keV distribute on one cascade region while higher energies generate defects distributed across multiple subbranches of the cascade.

In more recent work, Teunissen *et al.* incorporated the effect of electronic stopping in their MD simulations of collision cascades in GaAs.[84] A recently proposed electron–phonon (EPH) model for nonadiabatic dynamics was used in this work, which treats the electron–phonon coupling and electronic stopping as two features of the same physical process. The evolution of the number of defects from the EPH-MD simulations is shown in Fig. 6. The relative number of defects from 1 to 10 keV increases by approximately a factor of 10, which is in agreement with the MD simulations by Gao *et al.*[82] and Nordlund *et al.*[61] However, the absolute number of defects found by Gao *et al.*[82] is much higher while the number of defects reported by Nordlund *et al.*[61] is also higher but much closer to the EPH-MD values. In both of the cases of EPH-MD and the work of Nordlund *et al.*,[61] the number of antisites is an order of magnitude lower than the number of Frenkel pairs

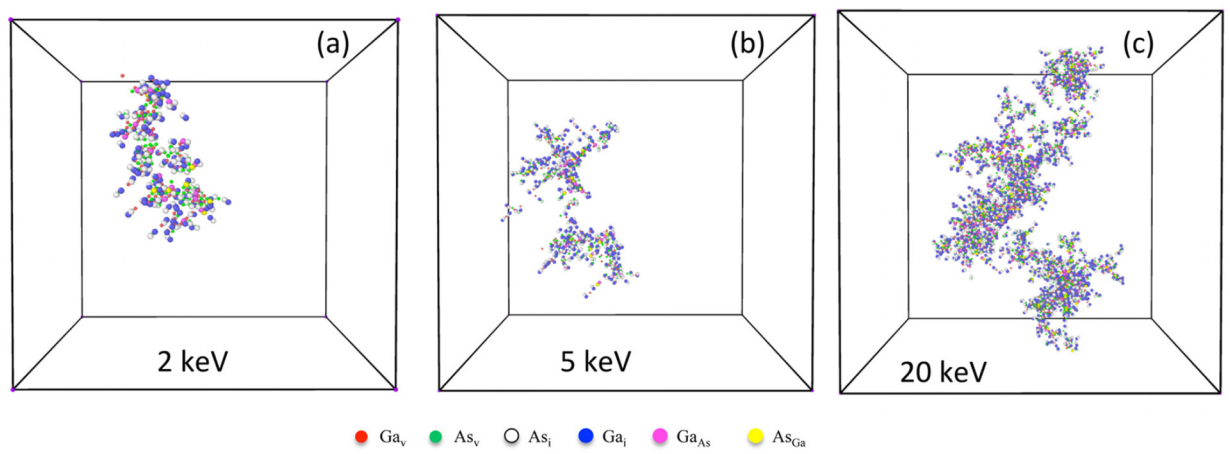

FIG. 5. The final defect states after (a) 2, (b) 5, and (c) 20 keV cascade in GaAs. The transition from a single pocket of atomic displacements to multiple subcascades is observed. Reproduced with permission from Gao *et al.*, J. Appl. Phys. 121, 095104 (2017). Copyright 2017 AIP Publishing LLC.[82]

(vacancies and interstitials). That the number of defects in all simulations is linear with PKA energy emphasizes the fact that getting the physics right even at the lowest energies is critical for meaningful predictions.

In Fig. 6, the EPH-MD values of the number of defects are also compared to the standard Norgett–Robinson–Torrens model (NRT)[85] formula, $N_{\text{defects}} = \frac{0.8E_{\text{PKA}}}{2E_d}$, where E_{PKA} is the PKA energy of recoil in the MD simulations, and E_d is the mean threshold displacement energy that is taken to be 13 eV, the average of the reported values for Ga and As.[86] The NRT model is a modified

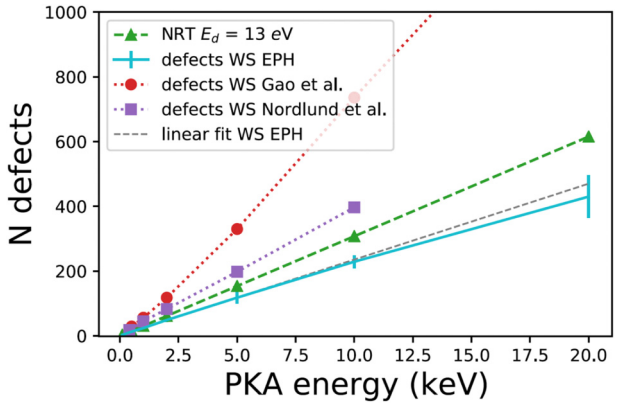

FIG. 6. Number of defects for multiple PKA energies from simulations by Teunissen *et al.*[84] Number of Frenkel pair defects as determined via the Wigner–Seitz (WS) method are compared with the numbers reported in Gao *et al.*[82] and Nordlund *et al.*[61] The number of defects as predicted via the NRT model $\left(N_{\text{defects}} = \frac{0.8E_{\text{PKA}}}{2E_d}\right)$ is evaluated with $E_d = 13$ eV. A fit to the number of EPH-MD defects at energies up to 5 keV is shown in gray, which has an effective E_d of 17.1 eV. Reproduced with permission from Teunissen *et al.*, Phys. Rev. Mater. **7**, 025404 (2023). Copyright 2023 American Physical Society.

Kinchin–Pease estimate for the total number of Frenkel pairs produced[61] and is based on the binary collision approximation (BCA). The number of defects from the EPH-MD simulations is only slightly smaller than predicted via the NRT model, as shown in Fig. 6.

C. The nonionizing energy-loss (NIEL) damage in GaAs

It has been observed that radiation damage in electronic components made from semiconductors or semiconducting compounds is proportional to the nonionizing energy loss (NIEL).[87] NIEL is a measure of the energy lost by a particle to nuclear recoils as it travels through medium. It disregards energy transfer that is used to liberate bound electrons. It, thus, represents the portion of incident energetic particles that is non-ionizing, and that affects the target material mainly by atomic displacements through inelastic nuclear scattering. The concept of NIEL is useful to describe problems concerning displacement damage and is commonly used as a metric to quantify a particular damage level due to radiation-induced atomic displacements.[87] NIEL differentiates between electron-only stopping (which just creates ionization) and nuclear stopping; however, the result of an atom displacement is a charged defect population. The formulation of NIEL can be determined through the Lindhard energy partition function $G(E)$,[88]

$$\text{NIEL} = \alpha \int_{E_d}^{E_{\max}} EG(E) \frac{d\sigma}{dE} dE, \tag{1}$$

where α is the atomic density of the target material, E is the kinetic energy of the recoil or energy of the primary knock-on atoms (PKAs), $E_{\max}$ is the maximum energy that can be transferred to a recoil nucleus by an incident particle, and E_d is the threshold displacement energy for GaAs. $G(E)$ is the Lindhard energy partition function to describe energy partitioning when an incoming particle interacts with a solid target. $\frac{d\sigma}{dE}$ is the differential interaction cross

section, which describes the probability of particle scattering or interaction with the target. Since the commonly used NRT formula relates the recoil energy to the number of defects through $N_{\text{defects}} = \frac{0.8E_{\text{PKA}}}{2E_d}$, Eq. (1) can also be expressed as

$$\text{NIEL} = \alpha \int_{E_d}^{E_{\max}} \frac{E_d}{0.4} N_{\text{defects}} G(E) \frac{d\sigma}{dE} dE. \quad (2)$$

Messenger and co-workers[25,53,89] have done substantial work involving the NIEL model for GaAs. They calculated NIEL as a function of particle energy for silicon ions and protons incident upon GaAs.[53] Gao *et al.*[82] used MD simulations to determine the accurate damage level by calibrating the NIEL model[25] in GaAs. Taking N_{defects} as obtained from MD simulations, Gao *et al.*[82] derived an "effective" NIEL for GaAs. Figure 7 presents the NIEL obtained based on MD results[82] for several different incident particles in GaAs, where the values of the NIEL calculated by an analytical approach[89] are superimposed for comparison. In general, the MD-informed NIEL values are a few times larger than the analytical NIEL values, particularly at higher energies (incident particle energies >1 MeV). However, due to the reduction in the number of defects predicted by standard MD by considering the effect of electronic stopping,[84] the comparison between the analytical NIEL formulation and MD based NIEL might suggest a more reasonable agreement.

V. SIMPLE INTRINSIC DEFECTS IN GaAs

In Sec. IV, we discussed how, during high-energy collision cascades in GaAs,[61,78,79] large damage regions form and consist of amorphous zones or vacancy and antisite clusters. However, even in the cases where amorphization is seen, the amorphous zones anneal out at room temperature, leaving behind a damage state consisting of small clusters of point defects, many of which can also be expected to anneal out easily.[61] These studies highlight the important role that isolated point defects and small defect clusters have in dictating the evolution of these materials in radiation environments. The isolated point defects include interstitials, vacancies, and antisites, and we call these as simple intrinsic defects in this paper. Among these defects, antisites are particularly relevant, as such defect requires high temperatures to anneal out.[78] Indeed, simple intrinsic defects and di-vacancies have been treated as the primary products of collision cascades in the model of defects and carrier transport in radiation-damaged GaAs in previous modeling study by Wampler and Myers.[90]

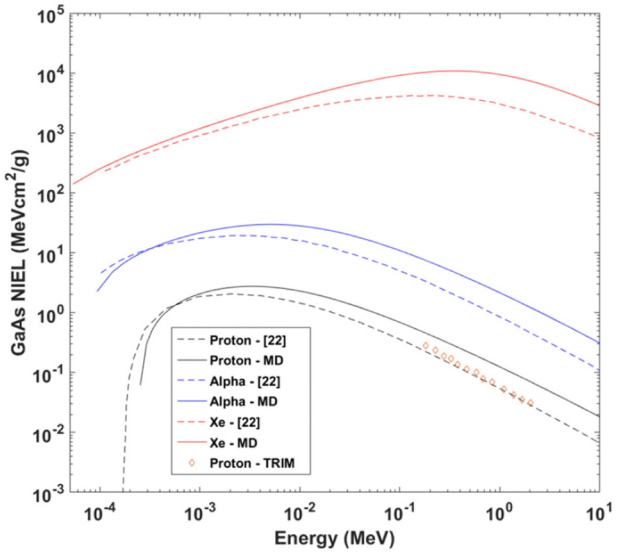

FIG. 7. The NIEL obtained based on the MD results[82] for several different incident particles in GaAs, where the values of the NIEL calculated by an analytical approach[89] are imposed for comparison. Reference 22 in the legend is Ref. 89 in this paper. Reproduced with permission from Gao *et al.*, J. Appl. Phys. 121, 095104 (2017). Copyright AIP Publishing LLC.[82]

Most of the native defects (grown crystal defects, excluding residual impurity and substitutional dopants) have been studied through electron irradiation experiments.[5] Earlier experimental studies[5] suggest that the native defects are not simple intrinsic defects. They were suggested to be defect complexes formed by pairing with other defects or with impurities. For example, even in the case of the *EL2* defect, which plays a major role in the electrical properties of bulk materials, it was thought to be the As antisite complexed with an As interstitial.[5]

The picture of these proposed defect models has largely changed as the result of later density functional theory (DFT) modeling studies. Schultz and Lilienfeld's DFT modeling[91] of simple intrinsic defects in GaAs provides an excellent explanation of the type of defect behavior that DFT calculations have revealed. In Schultz and Lilienfeld's DFT work,[91] it is demonstrated that in most cases, the so-called defect complex should not exist. In Fig. 8, their computed defect energy levels for simple intrinsic defects in GaAs are shown, where levels connected with vertical lines are negative-U defect-level systems. In negative-U defect level systems, the defect introduced into the semiconductor can trap two electrons (or holes) with the second bound more strongly than the first,[92] which is considered to be unusual, reflecting strong lattice relaxation effects upon capture and emission of carriers.[93] The defect gap states are important since they greatly influence the recombination pathways and, thus, affect the electrical/optical performance of GaAs devices (see Sec. VII).

It should be noted that most of the DFT works covered in this section uses regular DFT exchange functionals such as the local density approximation (LDA) or the Perdew–Burke–Ernzerhof functional within the generalized gradient approximation (PBE-GGA) or PBE-GGA. In general, higher level DFT calculations such as hybrid functionals are more accurate, but currently have only been applied in studies of antisites and vacancies in GaAs.[94,95]

A. The arsenic and gallium antisites (As_{Ga}, Ga_{As})

DFT work[91,94–98] shows that an isolated neutral arsenic antisite As_{Ga} corresponds to *EL2* in the DLTS of GaAs samples. As shown in Fig. 9, As_{Ga} has a metastable configuration, which is a complex of an As interstitial and a Ga vacancy. This metastable configuration deviates from the standard As_{Ga} antisite structure [Fig. 9(b)] by the substitutional As retreating along a [111]

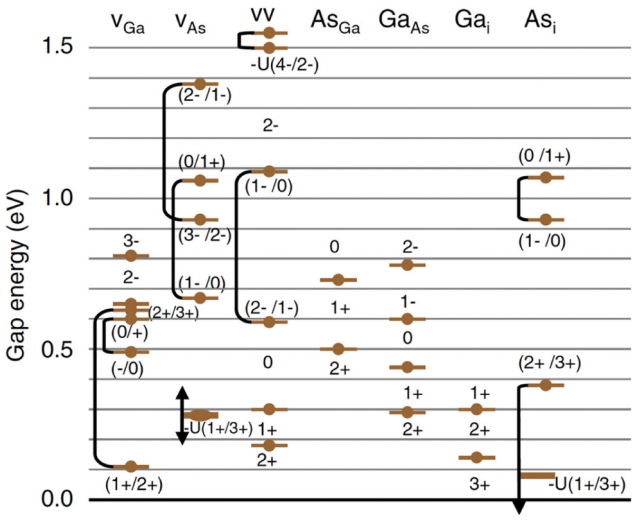

FIG. 8. Computed PBE defect energy levels for simple intrinsic defects in GaAs, plus di-vacancy cluster, extrapolated to infinite supercells from results of 216-site supercell calculations.[91] Levels connected with vertical lines are negative-U defects. Reproduced with permission from Schultz and von Lilienfeld, Modelling Simul. Mater. Sci. Eng. **17**, 084007 (2009). Copyright 2009 IOP Publishing.

direction toward an open interstitial site [Fig. 9(c)]. This metastable site is 0.43 eV higher than the As_{Ga} antisite ground state configuration and has a transition barrier of 0.18 eV to the saddle configuration.[91] The computed midgap As_{Ga} (0/+) donor state, at 0.80–0.81 eV below the conduction band (CB) minimum,[91] is consistent with experimental observations for the *EL2* (0/+) level, ranging from 0.74 to 0.83 eV below the CB edge.[99–102] In Fig. 9(b), the As

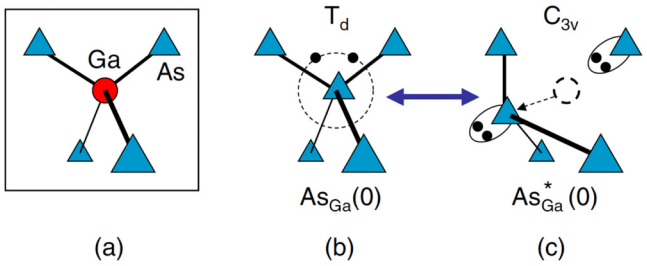

FIG. 9. Schematic depiction of the bonding around the arsenic antisite As_{Ga} and its metastable configuration As^*_{Ga}. A Ga atom in the perfect crystal[91] (a) is substituted by an arsenic atom to form (b) the ground state As^0_{Ga}. The two extra valence electrons of the As atom (with respect to the Ga atom it replaces) orbit the center in a localized Rydberg (non-bonding) state. In the metastable state (c), the substitutional As retreats along a [111] direction toward an open interstitial site, breaking one As–As bond, and straining the others. The two extra electrons are captured in the dangling bonds, forming complete lone pairs; the electron affinity of the lone pairs compensating for the energy cost of breaking the bond and introducing local strain. Reproduced with permission from Schultz and von Lilienfeld, Modelling Simul. Mater. Sci. Eng. **17**, 084007 (2009). Copyright 2009 IOP Publishing.

has more than two electrons that can be accommodated in the bonds to its neighbors (two electrons more than the original Ga host atom that occupied the site), making it a double donor.

In contrast to As_{Ga}, the gallium antisite Ga_{As} is expected to be a double acceptor. Zhang and Chadi,[103] in their DFT calculations, suggested that Ga_{As} possesses strong structural bistabilities as a function of the Fermi-level position in the bandgap. In addition, it forms low-energy metastable complexes and undergoes exchange reactions with mobile As interstitials. As a result of the exchange reaction, the gallium antisites are transformed into GaAs bulk, releasing Ga interstitials.

B. The gallium and arsenic interstitials (Ga_i, As_i)

Ga interstitials (Ga_i) in GaAs are more studied than As interstitials (As_i) in the literature. After numerous experimental and theoretical efforts to understand the behavior of Ga_i, there is still some uncertainty. On the experimental side, while Ga_i in GaAs has never been directly observed, the diffusion of Ga_i in GaAs has been probed using zinc diffusion experiments. Bösker *et al.*[104] found that Ga_i diffusion profile can be described by the +2 and +3 charge states of Ga_i. However, later experimental works by Bracht *et al.*[105,106] found in similar experiments that the diffusion is mainly mediated by neutral and singly positively charged Ga_i.

On the theoretical side, Malouin *et al.*[107] was the first to present a detailed study of many of the possible configurations of Ga_i using DFT modeling. As shown in Fig. 10, their study showed that, from a total of eight possible configurations, half of them are not stable. The work of Schultz and von Lilienfeld[91] suggested that Ga_i will diffuse in its positive charge states (+1, +2, and +3), with a migration barrier of $\geq$1 eV, which contradicts the conclusion of Bracht *et al.*[105,106] A later DFT work by Schick and Morgan[108] found that the migration path may depend on the Fermi level in the material system, and the neutral split configuration of Ga_i could contribute significantly to the diffusion process with a barrier of much less than 1 eV, for certain Fermi-level range. However, one caveat of the Schick and Morgan work[108] is that they did not use any energy corrections in their charged state calculations.

For As interstitials, there is less inconsistency. Using DFT, Wright and Modine[109] have studied the migration process of the As interstitial. Their calculated migration energy for the migration of the +1 As_i (0.45 eV) is in good agreement with the measured value (0.5 ± 0.15 eV) in p-type GaAs.[110] Wright and Modine's study[109] also suggested that under current injection As_i could migrate through a modified Bourgoin–Corbett process[111] with a very small migration barrier of 0.05 eV, making it nearly an athermal transport process.

In the Bourgoin–Corbett process,[111] capture of a minority carrier changes the defect state from a stable state to a migration transition state, causing the defect to transform to a new stable state shifted in position from the original state. When this new defect state captures a majority carrier, it again changes from a stable state to a migration transition state causing the defect to transform back to the original stable state, possibly at a new position. By alternately capturing minority and majority carriers, the defect can, thus, migrate through the lattice. This process is different from standard diffusion mechanism, in that the successive changes in a defect charge state dominate the migration process. It

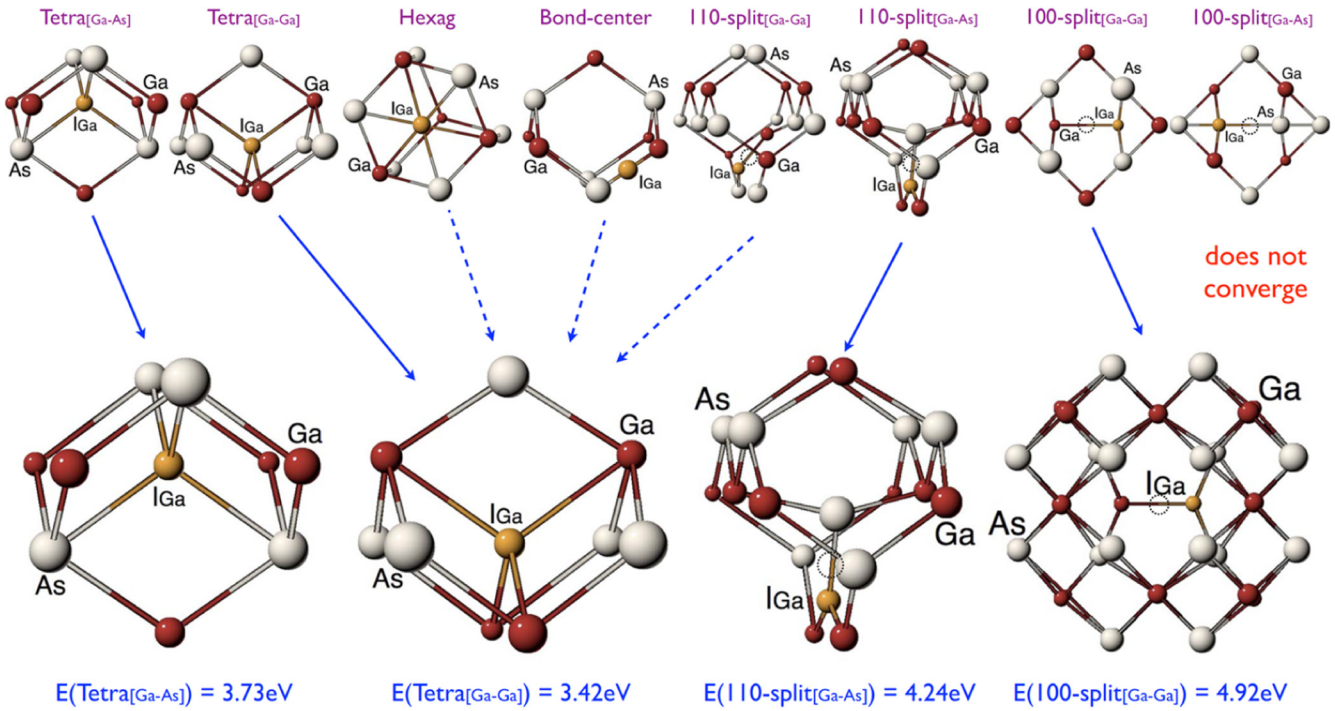

FIG. 10. Top: The eight initial configurations considered in the study[107] of the neutral self-interstitial Ga_i (denoted as I_{Ga} in the figure). The first six configurations, going from left to right, are viewed along the ⟨110⟩ direction, while the remaining two are viewed along the ⟨100⟩ direction. Bottom: The metastable configurations obtained after full relaxation of Ga_i. Full arrows connect the initial configuration to its metastable counterpart, while dashed arrows mean that the initial configuration is unstable and converged to the pointed configuration. Gallium atoms are red, while arsenic atoms are white; the interstitial Ga atom is colored yellow. For split interstitial structures, regular sites of the displaced lattice atoms are highlighted by a dotted circle. Reproduced with permission from Malouin *et al.*, Phys. Rev. B **76**, 045211 (2007). Copyright 2007 American Physical Society.

can arise as the dominant process under certain conditions, e.g., in Barnes's report[112] that radiation damage in a GaAs laser diode could be annealed at low temperatures by carrier injection (i.e., under forward bias).

C. The gallium and arsenic vacancies (V_{Ga}, V_{As})

In early DFT work, Baraff and Schlüter[113] discovered that the gallium vacancy (V_{Ga}) could be structurally bistable as a function of charge state, which was later studied in detail by Pöykkö *et al.*[114] This finding was also confirmed by Schultz and Lilienfeld.[91] Gallium vacancy takes both the form of a single gallium vacancy, and a form of where a neighboring arsenic atom shifts in the vacant gallium site, creating a nearest neighbor As vacancy–As antisite pair. The latter kind of structure is also seen in oxides.[115–117] There is significant consensus from numerous studies that the single gallium vacancy structure takes the charge states from +1 to −3.[91,118–120] However, for the positively charged gallium vacancy, the site-shifted form becomes important.

El-Mellouhi and Mousseau[121] carried out DFT study of the charge-dependent migration pathways for the single Ga vacancy in GaAs, from neutral to −3 charge states. The self-diffusion process is dominated by jumps to the second nearest Ga neighbors to reach the same sublattice. Their results suggested that for a diffusion path to second nearest neighbors (Ga neighbor), the migration barrier for V_{Ga} is 1.7–2.0 eV from neutral to −3 charge states. Bliss *et al.*[122] measured the migration barriers for Ga vacancies in low-temperature GaAs using the positron annihilation technique. Analysis of annealing kinetics gives a migration barrier of 1.5 ± 0.3 eV for vacancy diffusion to second nearest neighbor sites (Ga neighbor).[122] Such experimental measurements agree with the DFT modeling values within the experimental error bars.

Like V_{Ga}, the arsenic vacancy (V_{As}) exhibits a site-shift bistability as a function of charge states.[91,123] El-Mellouhi and Mousseau[124] also studied the As vacancy diffusion pathway. They found that the diffusion path is essentially insensitive to the charge state, with a migration barrier of 2.38 eV for the −1 charge state and 2.41–2.44 eV for the +1 charge state. In general, arsenic vacancies are less mobile than gallium vacancies because of higher diffusion barriers. It was estimated that arsenic vacancies should, therefore, diffuse 4500 times slower than Ga at 1000 K.[124]

VI. DEFECT CLUSTERS IN GaAs

It is evident from earlier sections that a complete understanding of defect clusters—defect structures that are comprised of more

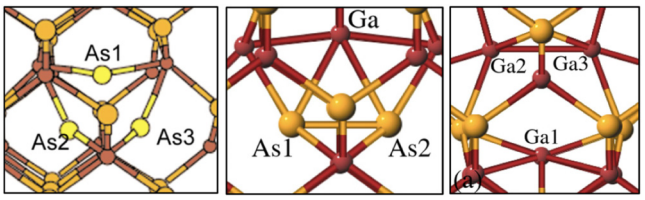

FIG. 11. Structure of As_{2i}, Ga_iAs_i, and Ga_{2i} di-interstitial clusters.[126] Reproduced with permission from Zollo *et al.*, J. Phys.: Condens. Matter **16**, 8991 (2004). Copyright 2004 IOP Publishing.

than one elementary point defect—and their evolution is essential for accurate modeling of radiation-induced defects and their impact on the microstructure in irradiated GaAs. This section consists of a brief overview of past research on interstitial and vacancy clusters in GaAs under irradiation. Even larger extended defects such as dislocations or (111)-oriented extended defect complexes are not covered due to lack of sound and quantitative results in the literature. These structures are, however, expected to impact device performance and are worthy of future study.

A. Interstitial clusters

Interstitial clusters are important clusters in defect evolution since the interstitials are the most mobile defects in GaAs. Zollo and co-workers[125–131] studied interstitial clusters in GaAs using both DFT and tight-binding (TB) MD. The most stable structures identified with DFT for the neutral di-interstitial clusters As_{2i}, Ga_iAs_i, and Ga_{2i} are shown in Fig. 11 (a different nomenclature, I_n, is also used at times, to label interstitial clusters made of n interstitials). For As_{2i}, it involves three As atoms sharing one As site. For Ga_iAs_i, it is composed of one As ⟨110⟩ dumbbell and one extra Ga in the closest tetrahedral site. For Ga_{2i}, it is composed of three Ga atoms sharing one Ga lattice site, with two of the Ga atoms form a ⟨110⟩ dumbbell while the third is very close to the tetrahedral site. These structures have C_{1h} (As_{2i}) and C_{2v} (Ga_iAs_i, and Ga_{2i}) symmetry, respectively.

All the di-interstitials exhibit high binding energies, as listed in Table I (negative value for attractive binding), indicating that the interstitial aggregates are readily formed from migrating isolated interstitials. In addition, Zollo and Gala[130] also studied the migration path of As_{2i} and Ga_iAs_i interstitial clusters and found these two di-interstitials have fairly low migration energy barriers: 0.76 eV for As_{2i} and 0.32 eV for Ga_iAs_i. It should be emphasized that these results are for neutral clusters and that, in principle, the clusters can have varying charge state just like the individual point defects.

Zolo and Gala[127,129] also studied larger interstitial clusters from I_3 to I_7 in GaAs, using tight-binding molecular dynamics (TBMD). The binding energies of these clusters are also listed in Table I. They have checked for the existence of low-energy reaction paths where the growth of larger clusters occurs through the capture of I_1 and I_2 by a pre-existing stable complex. In addition, the I_5 ground state configuration ($Ga_{2i}As_{3i}$) was found to be the most stable I_n complex as compared to its neighbors (I_4 and I_6). It was suggested that I_5 is the nucleation seed for (111)-oriented extended defect complexes in GaAs, such as dislocations or stacking faults.[129]

TABLE I. The binding energy and migration barrier of interstitial clusters. Tight-binding results are marked with an asterisk and the remainder are calculated with DFT. Values are taken from the indicated references.

	Binding energy (eV)	Migration barrier
Ga_{2i}	−1.46[126]	…
As_{2i}	−2.35[126]	0.76 eV[130]
Ga_iAs_i	−2.24[126]	0.32 eV[130]
As_{3i}[a]	−1.87[127]	…
Ga_{3i}[a]	−2.66[127]	…
$Ga_{2i}As_i$[a]	−3.73[127]	…
$Ga_{2i}As_i$[a]	−4.65[129]	…
$Ga_{2i}As_{2i}$[a]	−6.95[129]	…
$Ga_{2i}As^*_{3i}$[a]	−9.31[129]	…
$Ga_{3i}As_{3i}$[a]	−10.36[129]	…
$Ga_{4i}As_{3i}$[a]	−12.34[129]	…

[a]Tight-binding results.

B. Vacancy clusters

Vacancy clusters are usually created during cascade collision displacements such as those that occur during neutron or ion irradiation. There has been some debate whether defects generated under electron irradiation like di-vacancies could be formed in GaAs.[132] Indeed, in an early positron annihilation study of electron irradiated GaAs,[132] the di-vacancy was thought not to exist, as supported by earlier DFT calculations of the positron annihilation lifetime.[133] However, recent DFT work by Schultz[132] suggested that *E*1 and *E*2 DLTS centers in the electron irradiated experiments are electronic signatures from di-vacancies. This is mainly due to the −3 and −4 charge state of the divacancy defect, which were not included in the earlier work,[133] leading to smaller positron annihilation lifetime.

Staab *et al.*[134] also studied the stability of various atomic arrangements of vacancy aggregates in GaAs, using a self-consistent-charge density-functional-based tight-binding method. They found that the first such stable aggregate is made up of 12 vacancies. They also calculated the positron lifetime of these clusters and found good agreement with the long positron lifetime component of about 500 ps measured in GaAs.[134]

Through various studies of defects in GaAs, it is clear that antisites typically have greater stability than other point defects. The interstitial defects are very mobile, even at room temperature. The vacancy defects are somewhat mobile, generally requiring higher than the room temperature to move. These defects are known to affect the electrical/optical performance of GaAs devices by defect-medicated carrier recombination pathways under operating conditions, a topic that will be covered in Sec. VII.

VII. CHARGE CARRIER DYNAMICS AND DEFECTS

The dynamics of charge carriers with lattice defects in GaAs is governed by the Coulomb force. Defects perturb the periodic

potential in the crystal lattice. This perturbation often results in regions of localized charge that can "capture" free carriers, leading to the formation of bound quantum states known colloquially as "traps." Traps may be individual point defects or defect complexes and may capture either electrons or holes. These traps are typically classified based on their binding energy and capture cross section. In many GaAs technological applications, traps play a crucial role in determining the recombination and transport properties of the device.[41,135] This fact reinforces the need to understand the defect structure in these materials, as outlined in Secs. I–VI.

A key piece of the carrier-defect dynamics in GaAs is the time a carrier spends captured, which depends on a ratio of the energy necessary to release the carrier from the bound state and the energy sources available to liberate it.[136,137] Because many defect states in GaAs are located near the band edge, quiescent thermal energy may be enough to liberate a charge from a bound state. Shallow traps, with energies close to the conduction or valence bands (such as gallium vacancies), can release carriers back into the bands relatively quick (~1 ns), whereas deep traps (such as arsenic antisites), situated closer to the middle of the bandgap, can hold carriers for much longer periods (~100 ns), significantly impacting GaAs's electronic and optical properties.[138]

The modern understanding of carrier-defect interaction in GaAs is considered as a transition between two quantum states. The states differ in their distribution of occupancy across the total spectrum of available energy levels, but do not change the spectrum (in the lowest order theories[139]). Carrier transitions can lead to the annihilation (or creation) of electron–hole pairs. Conservation of energy dictates that, with the annihilation of electron–hole pairs, the energy must be released as light, lattice vibrational energy, or additional kinetic energy of the existing carrier population. These energy pathways are often called radiative, non-radiative, and Auger processes, respectively (see Fig. 12).

Radiative transitions in GaAs are critical to optoelectronic device performance in radiation environments and involve the emission or absorption of photons as carriers transition between energy states. When an electron in the conduction band recombines with a hole in the valence band, the energy difference between these states can be released as a photon, resulting in radiative recombination.[141] The efficiency of the radiative transition depends on factors, such as the bandgap energy, the density of states, and the overlap of electron and hole wavefunctions. The radiative process is fundamental to the operation of light-emitting devices such as LEDs and semiconductor lasers.[142] Understanding how defects affect this process is crucial for improving the performance of GaAs-based optoelectronic devices, and ultimately, designing radiation-tolerant material systems.

In addition to photon-mediated transitions, charge carriers have been shown to interact with defects through multi-phonon relaxation pathways in GaAs.[138,143] This process involves the non-radiative transfer of energy from the trapped carrier to the lattice in the form of phonons [Fig. 12(b)].[144] Multi-phonon relaxation is particularly significant for deep traps (like those associated with the arsenic antisite in GaAs) where the energy difference between the trapped state and the conduction or valence band edge is too large to be bridged by single-phonon process.[35,145] It is also a driving mechanism for transitions between electronic states with large momentum disparity, as the photon momentum is vanishingly small compared to the electron momentum.[146] The probability of multi-phonon relaxation depends on the coupling strength between the electronic states and the phonon modes, which is influenced by the local atomic structure and bonding characteristics around the defect. Although it results in a very different energy balance, phonon-mediated transitions are still fundamentally driven by the Coulomb interaction if the defect is charged. Modern work has leveraged this understanding to suppress phonon-mediated non-radiative decay channels in GaAs-based optoelectronic devices.[147]

For non-radiative recombination, in the literature, carrier capture processes are often described in terms of capture cross sections σ. In first-principles DFT computational works, the capture coefficients, C, as defined as in the work of Alkauskas *et al.*,[143] are calculated. The two quantities are related via $C=\langle \upsilon \rangle \sigma$, where $\langle \upsilon \rangle$ is the average thermal velocity of carriers. In a recent work,[138] the capture coefficients of various point defects in GaAs were calculated using a first-principles-based theory of multi-phonon emission. Further work is needed for the calculation of the capture coefficient of more extended clusters in GaAs.

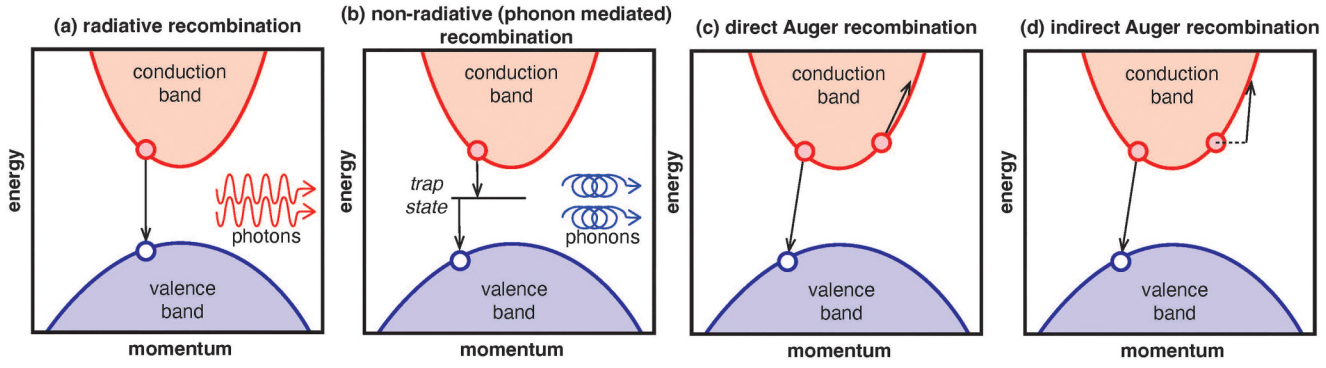

FIG. 12. Schematics for (a) radiative recombination, (b) non-radiative recombination, (c) direct Auger recombination, and (d) indirect Auger recombination. (c) and (d) are adapted from Ref. 140. Reproduced with permission from Steiauf *et al.*, ACS Photonics **1**, 643–646 (2014). Copyright 2014 American Chemical Society.

Last, Auger processes are non-radiative recombination mechanisms where the energy released by an electron–hole recombination is transferred to a third carrier (another electron or hole) rather than emitting a photon. This third carrier is excited to a higher energy state through its interaction with the electron–hole plasma. The Auger recombination rate is highly dependent on the carrier density, typically increasing with the cube of the carrier concentration.[140] This makes Auger processes particularly significant in heavily doped semiconductors or under high injection conditions, such as in high-power laser diodes. There has been a long history of investigating the effects of Auger recombination in GaAs, specifically as a function of carrier concentration.[41,140,148–153] Auger recombination can lead to significant efficiency losses in GaAs-based optoelectronic devices, as the energy is dissipated as heat rather than light when the excited carriers ultimately decay via intraband phonon-mediated processes.

The relative efficiency of all these interactions affects the overall recombination dynamics in GaAs. Performance is directly linked to radiative recombination processes. Non-radiative recombination via traps and multi-phonon relaxation pathways can significantly reduce the carrier lifetime and mobility,[15] thereby impacting the performance of GaAs devices. Understanding these fundamental interaction dynamics is essential for describing and predicting radiation damage effects in devices where charge carrier dynamics are critical to device performance such as GaAs photovoltaic cells, light-emitting diodes, and laser diodes. However, there is one more important situation to discuss, and that is the scenarios involving significant random disorder, where the localization effects of carrier wave functions are important.

Wave function localization significantly affects the rates at which carriers are captured by defects or emitted back into the conduction and valence bands.[138,154] When a carrier's wave function overlaps with a defect wavefunction (in such a case, the wavefunction of defects is delocalized), the probability of capture increases, potentially leading to enhanced non-radiative recombination rates.[155] Conversely, if carriers are spatially separated from defects due to wave function localization, the capture rate decreases, potentially reducing non-radiative recombination pathways. This localization effect is crucial in understanding the efficiency of GaAs light-emitting devices, photovoltaic cells, and other semiconductor applications where minimizing carrier capture by defects is essential.[56,156–158]

In nanoscale semiconductor structures, such as quantum dots or nanowires, quantum confinement leads to discrete energy levels and localized wave functions. This is due to the dimensional confinement of carriers and/or defects. Localization phenomena can significantly influence carrier interaction with surface defects or interface states,[159,160] impacting recombination pathways and overall device performance. Understanding and controlling localization phenomena is essential to achieve tailored device design, e.g., radiation-tolerant GaAs lasers.

In summary, modern semiconductor technologies fundamentally leverage quantum behavior to enable functionality—ultimately, the operation and performance of these devices starts at the quantum level. Consequently, further study of the many-body carrier-defect dynamics is crucial for advanced semiconductor device design and radiation-tolerant device development. Fundamental defect properties, such as carrier trap energy, influence the recombination rates and efficiency of devices like LEDs and laser diodes. Similarly, the capture cross section is vital for understanding carrier dynamics and non-radiative recombination processes. A larger capture cross section indicates a higher likelihood of carriers being trapped, which can significantly affect the carrier lifetime and overall device performance. By accurately determining these parameters, device architectures can potentially be tuned to enhance efficiency, reduce energy losses, and improve the operational stability of optoelectronic devices in harsh radiation environments.

VIII. GAPS AND CHALLENGES TOWARD UNDERSTANDING OF DEFECTS EVOLUTION IN GaAs

The previous discussion has highlighted the significant progress that has been made in understanding non-equilibrium defects and their associated impact on performance in GaAs. However, despite the decades of research in this material, there are still many outstanding questions that limit our ability to fully describe and ultimately predict the properties of GaAs under irradiation. There are several gaps in our present understanding of defects evolution in GaAs, and one possible challenge in modeling that evolution:

(a) Despite extensive investigation on the simple intrinsic defects in GaAs at the DFT scale, there is still ambiguity in terms of a consistent picture of the thermokinetic description of defects in GaAs. This is mostly due to the underestimation of the bandgap within regular DFT at either LDA or GGA levels. Employing hybrid functionals, such as HSE[161] or PBE0,[162] are expected to fill this gap.
(b) Radiation-induced defect evolution is inherently a non-equilibrium problem. The defect clusters could play a significant role in determining that evolution, depending on irradiation conditions. However, the impact of defect clusters on the evolution of radiation damage has not been explored. We suggest that the prediction of defect evolution could employ the cluster dynamics[163,164] approach to solve the myriad of coupled differential equations that describe defect transport and reactions under non-equilibrium conditions. The strength of cluster dynamics is that it can account for hundreds of distinct defect species, including electronic defects, and solve for their coupled evolution over time. This approach has been successfully applied to a variety of radiation damage problems including for metals and ceramics,[165,166] particularly nuclear fuels,[167,168] and has been able to utilize atomistic data to quantitatively compare to experimental measurements under irradiation.
(c) Linking of defect content and evolution to the performance degradation of GaAs optoelectronics is in general lacking. While there has been some encouraging progress in this area in modeling space-based infrared imaging devices,[169] which couples MD and a defect diffusion-reaction model with a space-weather-forecast model, more general capabilities are lacking. A multi-scale approach to simulate the defect evolution profile and combine the radiation damage simulations to the optical performance modeling of optoelectronics is still non-existent.

(d) It is well known that in both Si and III–V materials, including GaAs, radiation can induce amorphization pockets and zones. Indeed, decades of effort have been devoted to understanding the amorphization process and the detailed structure of the amorphous phase.[64,170–172] However, the fact that these materials readily amorphized under irradiation poses challenges to fully simulate the microstructural evolution process at the atomistic level. In particular, during irradiation under operating conditions, amorphization will be a dynamic process, with regions of the material amorphizing and recrystallizing, a process that can be further aided by irradiation[172,173] and which can be a source of point defects.[174] These local regions of amorphous material can further act as sinks for defects.[175] While these "pockets" are known to impact the overall damage evolution in semiconductors and their incorporation into models is critical for predicting amorphization thresholds,[176] there is still a need to more fully understand their dynamic evolution and their interaction with mobile crystalline defects. High fidelity models to describe how amorphous regions transform under thermal annealing and how this process may affect defect evolution are still not available for materials beyond Si.

These are only a few of the gaps that remain in our knowledge of radiation effects in GaAs. There are a number of other questions that need to be addressed. For example, what are the recombination pathways for non-equilibrium defects in GaAs? It has been shown in another semiconductor, SiC, that there are extra barriers for recombination that impede defect annihilation.[177] Is the same true in GaAs? Another consideration is the fact that GaAs is not used as a pure material; it is often doped to reasonably high levels to induce functionality. How those dopants interact with defects, possibly acting as diffusion traps or nucleation sites, is unclear. In this review, we have focused on defects induced by displacement damage, but ionizing radiation can create, at least transiently, electronic defects that can also impact performance. The lifetime of those defects is important to assess in order to determine how GaAs irradiated by, e.g., γ-rays will perform. Related to the amorphization question, other extended defects such as precipitates, dislocation loops, and vacancy clusters can form and will further impact the evolution and performance of the material.

Before we conclude, two additional related topics are also worth mentioning. One topic is the effect of radiation on the dielectric properties of GaAs. The dielectric function dictates, for example, the allowed electromagnetic modes in an optical device.

TABLE II. GaAs-based devices and radiation damage effect on components.

Material	Device	Radiation damage
GaAs (host)	Space solar cell, MOSFET, HEMT, HBT, photodiode, and laser diode.[183]	Radiation-induced defects reduce carrier mobility, lowering the device's efficiency (exposed to electron beams, 10–20 MeV up to 2 MGy).[184]
GaAs-related compound		
GaAsP	Material for manufacturing red, orange, and yellow LED[185,186] and solar cell.	Decrease in the intensity of luminescence and increase in the differential resistance of the diodes (irradiated by 2 MeV electron with fluences of 2.6×10^{16} e/cm^2).[187]
AlGaAs	Space solar cell, LED,[185] and laser diode.[188]	Radiation damage leads to increased non-radiative recombination, reducing quantum efficiency and resulting in light loss [irradiated by 14 MeV neutron with fluences of 4×10^{14} n/cm^2 (1 MeV)].[189]
InGaAs	Photodetector,[190,191] space solar cell, HEMT,[192] and VCSEL.[193]	Radiation damage increases non-radiative recombination, reducing current conduction efficiency and overall device performance. In high-frequency/high-power applications, these defects can decrease device stability. Lower radiation tolerance compared to InGaP (irradiated by 1 MeV electron with 10^{16} e/cm^2),[194] (24 GeV proton up to 1.1×10^{16} p/cm^2).[195]
InGaP	HEMT, HBT, VCSEL, space solar cell.[196,197]	Suffering from radiation-induced degradation.
GaAsSb	HBT, photodiode, VCSEL, laser diode,[194] multi-junction solar cell.[198]	Changes in noise fluctuations and current–voltage characteristics (under gamma ^{60}Co exposure, 500 kGy).[24]
InGaAsP	Photodiode,[199] multi-junction solar cell,[200] LED,[201] waveguide, laser diode.[202]	Radiation-induced lattice defects, leading to reduction of the non-radiative recombination lifetime and of the carrier mobility due to scattering (irradiated by 1 MeV electron with 10^{16} e/cm^2, and 1 MeV neutron up to 10^{16} n/cm^2),[203] (2 MeV and 30 MeV proton up to 5×10^{12} p/cm^2 and reactor neutron up to 10^{12} n/cm^2).[204]
Insulating dielectric/buffer layer		
Al_2O_3	HEMT gate oxide, Insulation for GaAs-based power devices and laser diodes.	Creating carrier traps in the Al_2O_3 layer [10 keV x rays up to 1000 krad (SiO_2)],[205] electric charging of bulk regions causes dielectric breakdown, and radiation-induced luminescence (8 MeV proton up to 7.3 MGy).[206]
MgO	MIS diode, buffer layer on the GaAs substrate.	Small shifts in its crystalline structure or color changes but dielectric strength and thermal conductivity are largely unaffected by radiation exposure.

In GaAs, and other similar materials, there is little known about how defects impact the dielectric properties of the material. The dielectric tensor function $\epsilon_{ij}(\omega)$, also known as the permittivity, is essential for accurately calculating the optical properties of any material. Żukowski *et al.*[178] measured the dielectric permittivity of GaAs after H^+ irradiation, showing that the dielectric permittivity increased as a function of temperature while remaining relatively constant in the sampled frequency range. Papež *et al.*[179] characterized the dielectric function of a GaAs-based photovoltaic cell after γ-ray irradiation. They found that the average value of the dielectric function decreased after irradiation and the location of the dielectric peaks shifted to a lower frequency. On the theoretical side, limited work has been done to calculate the effect of defects on the dielectric function of GaAs from first principles. Guo *et al.*[180] used GGA on a 64-atom supercell to calculate the dielectric properties of GaAs with vacancy, antisite, and interstitial intrinsic defects. No published work has been on the dielectric function of defective GaAs calculating using a larger supercell to better account for long range effects of the defect sites. Both the local field effect and the excited state energies could contribute to a more accurate calculation of the complex permittivity in GaAs. In addition, the reported dielectric relaxation time of 10^{-4} s,[181] a time scale of non-negligible, could be explored further by time-dependent DFT calculations. The relative sparsity of theoretical work in this area on GaAs provides further study opportunity.

Another related topic is the impact of radiation on the heterogeneous integration of GaAs with other materials in modern device architecture. In modern device architectures, GaAs is often integrated with other materials in multi-layer or heterojunction structures. For example, the combination of GaAs with materials, such as AlGaAs or InGaP, produces efficient light emission (in LEDs and lasers) and light absorption (in photodetectors and photovoltaic cells).[182,183] These modern device architectures allow GaAs-based technology to achieve high performance, reliability, and/or energy conversion efficiency, meeting the demands of high-frequency (above 1 GHz), high-power, high-bitrates and high-speed telecommunications and other optoelectronic applications.

Radiation exposure can deteriorate the performance of the semiconductor devices, causing a degradation in output, reliability, or light emission/absorption efficiency, leading to potential failure if the device is exposed to high radiation environment over time. When irradiation impacts GaAs and hetero-integrated materials, GaAs and the integrated materials develop defects, which can negatively affect the performance of the entire device. The integrated materials forming heterojunctions include aluminum gallium arsenide (AlGaAs), indium gallium arsenide (InGaAs), gallium arsenide phosphide (GaAsP), Indium gallium phosphide (InGaP) grown on GaAs substrates, gallium arsenide antimonide (InGaSb), and indium gallium arsenide phosphide (InGaAsP). The devices manufactured with these materials include laser diodes, LEDs, photodiode, photodetectors multi-junction solar cells, high electron mobility transistors (HEMTs), vertical-cavity surface-emitting lasers (VCSELs), heterojunction bipolar transistors (HBTs), microwave frequency integrated circuits (ICs), quantum well and quantum dot lasers, etc. In Table II, the effect of radiation on the GaAs-related compound semiconductor and its impact on the GaAs-based devices is listed.

IX. SUMMARY

In summary, the fundamental understanding of radiation-induced defects in GaAs is reviewed. Radiation-resilient optoelectronic materials are highly desired in space and nuclear applications, and understanding the relevant defects and electronic processes in GaAs is crucial for describing, predicting, and designing both current and next-generation applications. In this paper, experimental studies of irradiated GaAs are reviewed, with particular emphasis on electrical property characterization, DLTS for characterization of the electronic levels of defects, and irradiation-induced amorphization zones. On the other hand, MD simulations of radiation damage offer the examination of damage structures with atomistic details. The MD results are compared to the NIEL model prediction, which is commonly used to describe the damage level due to irradiation-induced atomic displacements. Most recent theoretical works, in particular, DFT-based calculations, focused on simple intrinsic defects and defect clusters in GaAs are also reviewed. These defects have an important role in dictating the evolution of GaAs material in radiation damage environments. The impact of radiation-induced defects on device behavior is through the coupled dynamics of charge carriers. It is envisioned that, by modeling of the above phenomena, device architectures can be tuned to enhance efficiency, reduce energy losses, and improve the operational stability of optoelectronic devices in harsh radiation environments. Finally, possible gaps and challenges toward understanding non-equilibrium defect evolution in GaAs are discussed.

ACKNOWLEDGMENTS

This work was supported by the Laboratory Directed Research and Development program of Los Alamos National Laboratory. Los Alamos National Laboratory, an affirmative action/equal opportunity employer, is operated by Triad National Security LLC, for the National Nuclear Security Administration of the U.S. Department of Energy under Contract No. 89233218CNA000001.

AUTHOR DECLARATIONS

Conflict of Interest

The authors have no conflicts to disclose.

Author Contributions

X.-Y. Liu: Conceptualization (equal); Writing – original draft (equal); Writing – review & editing (equal). **C. N. Singh:** Conceptualization (equal); Writing – original draft (equal); Writing – review & editing (equal). **E. R. Kennedy:** Writing – original draft (equal); Writing – review & editing (equal). **S. Huang:** Writing – original draft (equal); Writing – review & editing (equal). **S. P. Fluckey:** Writing – original draft (equal); Writing – review & editing (equal). **C. Matthews:** Writing – review & editing (equal). **B. P. Uberuaga:** Conceptualization (equal); Writing – original draft (equal); Writing – review & editing (equal).

DATA AVAILABILITY

The data that support the findings of this study are available from the corresponding author upon reasonable request.

REFERENCES

[1]R. N. Hall, R. O. Carlson, T. J. Soltys, G. E. Fenner, and J. D. Kingsley, "Coherent light emission from GaAs junctions," Phys. Rev. Lett. **9**, 366 (1962).
[2]R. Williams, "Determination of deep centers in conducting gallium arsenide," J. Appl. Phys. **37**, 3411 (1966).
[3]D. V. Lang, "Deep level transient spectroscopy—New method to characterize traps in semiconductors," Bull. Am. Phys. Soc. **19**, 298–299 (1974).
[4]D. V. Lang, "Recalling the origins of DLTS," Physica B **401–402**, 7–9 (2007).
[5]J. C. Bourgoin, H. J. Von Bardeleben, and D. Stiévenard, "Native defects in gallium-arsenide," J. Appl. Phys. **64**, R65–R92 (1988).
[6]V. M. Goldschmidt, "Crystal structure and chemical constitution," Trans. Faraday Soc. **25**, 253–0282 (1929).
[7]H. Welker, "Uber Neue Halbleitende Verbindungen," Z. Naturforsch. A **7**, 744–749 (1952).
[8]N. Okamoto, H. Kurebayashi, T. Trypiniotis, I. Farrer, D. A. Ritchie, E. Saitoh, J. Sinova, J. Mašek, T. Jungwirth, and C. H. W. Barnes, "Electric control of the spin Hall effect by intervalley transitions," Nat. Mater. **13**, 932–937 (2014).
[9]L. Q. Tian and W. Shi, "Analysis of operation mechanism of semi-insulating GaAs photoconductive semiconductor switches," J. Appl. Phys. **103**, 124512 (2008).
[10]S. T. Weir, Y. K. Vohra, C. A. Vanderborgh, and A. L. Ruoff, "Structural phase-transitions in GaAs to 108-GPa," Phys. Rev. B **39**, 1280–1285 (1989).
[11]J. W. Allen, "Gallium arsenide as a semi-insulator," Nature **187**, 403–405 (1960).
[12]S. M. Sze and K. K. Ng, *Physics of Semiconductor Devices* (John Wiley & Sons, 2006).
[13]Y. X. Wang and W. Windl, "Native point defects from stoichiometry-linked chemical potentials in cubic boron arsenide," J. Appl. Phys. **129**, 075703 (2021).
[14]R. Mishra, O. D. Restrepo, A. Kumar, and W. Windl, "Native point defects in binary InP semiconductors," J. Mater. Sci. **47**, 7482–7497 (2012).
[15]A. H. Johnston, "Radiation effects in optoelectronic devices," IEEE Trans. Nucl. Sci. **60**, 2054–2073 (2013).
[16]H. J. Kluge and W. Nörtershäuser, "Lasers for nuclear physics," Spectrochim. Acta B **58**, 1031–1045 (2003).
[17]I. Aharonovich, D. Englund, and M. Toth, "Solid-state single-photon emitters," Nat. Photonics **10**, 631–641 (2016).
[18]J. R. Srour and J. M. Mcgarrity, "Radiation effects on microelectronics in space," Proc. IEEE **76**, 1443–1469 (1988).
[19]H. Kressel, "The effect of crystal defects on optoelectronic devices," in *Semiconductors and Semimetals*, edited by R. K. Willardson and A. C. Beer (Elsevier, 1981), pp. 1–52.
[20]M. D. McCluskey and A. Janotti, "Defects in semiconductors," J. Appl. Phys. **127**, 190401 (2020).
[21]L. A. Coldren, S. W. Corzine, and M. L. Mashanovitch, *Diode Lasers and Photonic Integrated Circuits* (John Wiley & Sons, 2012).
[22]D. Y. Luo, R. Su, W. Zhang, Q. H. Gong, and R. Zhu, "Minimizing non-radiative recombination losses in perovskite solar cells," Nat. Rev. Mater. **5**, 44–60 (2020).
[23]S. J. Pearton, A. Aitkaliyeva, M. H. Xian, F. Ren, A. Khachatrian, A. Ildefonso, Z. Islam, M. A. Rasel, A. Haque, A. Y. Polyakov, and J. Kim, "Review-radiation damage in wide and ultra-wide bandgap semiconductors," ECS J. Solid State Sci. **10**, 055008 (2021).
[24]N. Papež, A. Gajdoš, R. Dallaev, D. Sobola, P. Sedlák, R. Motúz, A. Nebojsa, and L. Grmela, "Performance analysis of GaAs based solar cells under gamma irradiation," Appl. Surf. Sci. **510**, 145329 (2020).
[25]G. P. Summers, E. A. Burke, P. Shapiro, S. R. Messenger, and R. J. Walters, "Damage correlations in semiconductors exposed to gamma-radiation, electron-radiation and proton-radiation," IEEE Trans. Nucl. Sci. **40**, 1372–1379 (1993).
[26]H. J. Stein, "Electrical studies of low-temperature neutron- and electron-irradiated epitaxial normal-type GaAs," J. Appl. Phys. **40**, 5300 (1969).
[27]L. W. Aukerman, R. D. Graft, P. W. Davis, and T. S. Shilliday, "Radiation effects in GaAs," J. Appl. Phys. **34**, 3590 (1963).
[28]R. Zuleeg and K. Lehovec, "Radiation effects in GaAs junction field-effect transistors," IEEE Trans. Nucl. Sci. **27**, 1343–1354 (1980).
[29]A. B. Campbell, A. R. Knudson, W. J. Stapor, G. Summers, M. A. Xapsos, M. Jessee, T. Palmer, R. Zuleeg, and C. J. Dale, "Particle damage effects in GaAs JFET test structures," IEEE Trans. Nucl. Sci. **33**, 1435–1441 (1986).
[30]J. L. Mcnichols and W. S. Ginell, "Predicted effects of neutron irradiation on GaAs junction field effect transistors," IEEE Trans. Nucl. Sci. **17**, 52 (1970).
[31]J. G. Williams, J. U. Patel, A. M. Ougouag, and S. Y. Yang, "Carrier removal and changes in electrical-properties of neutron-irradiated GaAs," J. Appl. Phys. **70**, 4931–4937 (1991).
[32]R. Coates and E. W. J. Mitchell, "Optical and electrical effects of high-concentrations of defects in irradiated crystalline gallium-arsenide," Adv. Phys. **24**, 593–644 (1975).
[33]D. V. Lang and L. C. Kimerling, "Observation of recombination-enhanced defect reactions in semiconductors," Phys. Rev. Lett. **33**, 489–492 (1974).
[34]D. V. Lang and C. H. Henry, "Nonradiative capture and recombination at deep centers in GaP and GaAs by multiphonon emission," Bull. Am. Phys. Soc. **20**, 390 (1975).
[35]C. H. Henry and D. V. Lang, "Nonradiative capture and recombination by multiphonon emission in GaAs and GaP," Phys. Rev. B **15**, 989–1016 (1977).
[36]C. T. Sah, "Bulk and interface imperfections in semiconductors," Solid-State Electron. **19**, 975–990 (1976).
[37]S. T. Pantelides, "Electronic-structure of impurities and other point-defects in semiconductors," Rev. Mod. Phys. **50**, 797–858 (1978).
[38]R. J. Nelson and R. G. Sobers, "Minority-carrier lifetime and internal quantum efficiency of surface-free GaAs," J. Appl. Phys. **49**, 6103–6108 (1978).
[39]A. Mitonneau, A. Mircea, G. M. Martin, and D. Pons, "Electron and hole capture cross-sections at deep centers in gallium-arsenide," Rev. Phys. Appl. **14**, 853–861 (1979).
[40]R. M. Fleming, S. M. Myers, W. R. Wampler, D. V. Lang, C. H. Seager, and J. M. Campbell, "Field dependent emission rates in radiation damaged GaAs," J. Appl. Phys. **116**, 013710 (2014).
[41]M. Niemeyer, P. Kleinschmidt, A. W. Walker, L. E. Mundt, C. Timm, R. Lang, T. Hannappel, and D. Lackner, "Measurement of the non-radiative minority recombination lifetime and the effective radiative recombination coefficient in GaAs," AIP Adv. **9**, 045034 (2019).
[42]G. M. Martin, E. Estève, P. Langlade, and S. Makram-Ebeid, "Kinetics of formation of the midgap donor EL2 in neutron-irradiated GaAs materials," J. Appl. Phys. **56**, 2655–2657 (1984).
[43]G. M. Martin, A. Mitonneau, and A. Mircea, "Electron traps in bulk and epitaxial GaAs crystals," Electron. Lett. **13**, 191–193 (1977).
[44]A. Jorio, C. Rejeb, M. Parenteau, C. Carlone, and S. M. Khanna, "Radiation-induced carrier enhancement and intrinsic defect transformation in N-GaAs," J. Appl. Phys. **74**, 2310–2317 (1993).
[45]F. D. Auret, A. Wilson, S. A. Goodman, G. Myburg, and W. E. Meyer, "Electrical characteristics of neutron-irradiation induced defects in N-GaAs," Nucl. Instrum. Methods Phys. Res., Sect. B **90**, 387–391 (1994).
[46]D. Pons and J. C. Bourgoin, "Irradiation-induced defects in GaAs," J. Phys. C: Solid State Phys. **18**, 3839–3871 (1985).
[47]V. Swaminathan, "Defects in GaAs," Bull. Mater. Sci. **4**, 403–442 (1982).
[48]R. Wörner, U. Kaufman, and J. Schneider, "Electron-spin resonance of As_{Ga} antisite defects in fast neutron-irradiated GaAs," Appl. Phys. Lett. **40**, 141–143 (1982).
[49]A. Goltzene, B. Meyer, and C. Schwab, "Electron-paramagnetic resonance determination of the generation rate of As antisites in fast-neutron irradiated GaAs," J. Appl. Phys. **54**, 3117–3120 (1983).

[50]F. D. Auret, S. A. Goodman, G. Myburg, W. O. Barnard, and D. T. L. Jones, "Electrical characterization of neutron-irradiation induced defects in undoped epitaxially grown N-GaAs," J. Appl. Phys. **74**, 4339–4342 (1993).
[51]S. M. Khanna, C. Rejeb, A. Jorio, M. Parenteau, C. Carlone, and J. W. Gerdes, "Electron and neutron radiation-induced order effect in gallium-arsenide," IEEE Trans. Nucl. Sci. **40**, 1350–1359 (1993).
[52]S. T. Lai, D. Alexiev, and B. D. Nener, "Comparison between deep-level defects in GaAs induced by gamma, 1 MeV electron, and neutron-irradiation," J. Appl. Phys. **78**, 3686–3690 (1995).
[53]J. H. Warner, S. R. Messenger, R. J. Walters, G. P. Summers, M. J. Romero, and E. A. Burke, "Displacement damage evolution in GaAs following electron, proton and silicon ion irradiation," IEEE Trans. Nucl. Sci. **54**, 1961–1968 (2007).
[54]D. Kamburov, K. W. Baldwin, K. W. West, S. Lyon, L. N. Pfeiffer, and A. Pinczuk, "Use of micro-photoluminescence as a contactless measure of the 2D electron density in a GaAs quantum well," Appl. Phys. Lett. **110**, 262104 (2017).
[55]O. Arif, V. Zannier, F. Rossi, D. De Matteis, K. Kress, M. De Luca, I. Zardo, and L. Sorba, "GaAs/GaP superlattice nanowires: Growth, vibrational and optical properties," Nanoscale **15**, 1145–1153 (2023).
[56]B. H. Hamadani, M. A. Stevens, B. Conrad, M. P. Lumb, and K. J. Schmieder, "Visualizing localized, radiative defects in GaAs solar cells," Sci. Rep. **12**, 14838 (2022).
[57]H. Gnaser, B. Heinz, W. Bock, and H. Oechsner, "Surface modification of GaAs(110) by low-energy ion irradiation," Phys. Rev. B **52**, 14086–14092 (1995).
[58]V. M. Mikoushkin, "Formation of GaAs N nanofilm on GaAs by low energy N implantation," Appl. Surf. Sci. **257**, 4941–4944 (2011).
[59]S. Dhamodaran, N. Sathish, A. P. Pathak, D. K. Avasthi, R. Muralidharan, B. Sundaravel, K. G. M. Nair, D. V. SridharaRao, K. Muraleedharan, and D. Emfietzoglou, "Ion beam analysis of defects and strain in swift heavy ion irradiated InGaAs/GaAs heterostructures," Nucl. Instrum. Methods Phys. Res., Sect. B **254**, 283–288 (2007).
[60]J. H. Neethling, A. Janse Van Vuuren, E. J. Olivier, and P. A. Van Aken, "TEM and HAADF STEM imaging of dislocation loops in irradiated GaAs," Acta Phys. Pol. A **136**, 245–249 (2019).
[61]K. Nordlund, J. Peltola, J. Nord, J. Keinonen, and R. S. Averback, "Defect clustering during ion irradiation of GaAs: Insight from molecular dynamics simulations," J. Appl. Phys. **90**, 1710–1717 (2001).
[62]R. A. Brown and J. S. Williams, "Critical temperature and ion flux dependence of amorphization in GaAs," J. Appl. Phys. **81**, 7681–7683 (1997).
[63]M. W. Bench, I. M. Robertson, M. A. Kirk, and I. Jenčič, "Production of amorphous zones in GaAs by the direct impact of energetic heavy ions," J. Appl. Phys. **87**, 49–56 (2000).
[64]R. A. Brown and J. S. Williams, "Crystalline-to-amorphous phase transformation in ion-irradiated GaAs," Phys. Rev. B **64**, 155202 (2001).
[65]G. Vitali, G. Zollo, C. Pizzuto, D. Manno, M. Kalitzova, and M. Rossi, "Cross-sectional high resolution electron microscopy of Zn+ implanted and low-power pulsed-laser annealed GaAs," Appl. Phys. Lett. **69**, 4072–4074 (1996).
[66]T. Schober, J. Friedrich, and A. Altmann, "Proton implantation into GaAs—Transmission electron-microscopy results," J. Appl. Phys. **71**, 2206–2210 (1992).
[67]R. P. Sharma, R. Bhadra, L. E. Rehn, P. M. Baldo, and M. Grimsditch, "Crystalline to amorphous transformation in GaAs during Kr ion-bombardment—A study of elastic behavior," J. Appl. Phys. **66**, 152–155 (1989).
[68]D. Chowdhury and D. Ghose, "Formation of nearly defect-free nanoripples by sputtering of GaAs (001) surface at high temperature," Surf. Interfaces **17**, 100364 (2019).
[69]M. Saito, T. Nishida, N. Saitoh, N. Yoshizawa, T. Suemasu, and K. Toko, "Solid-phase crystallization of gallium arsenide thin films on insulators," Mater. Sci. Semicond. Process. **124**, 105623 (2021).
[70]Y. Wang, X. Guo, J. M. Wei, C. Yang, Z. J. Luo, J. H. Wang, and Z. Ding, "Effect of initial crystallization temperature and surface diffusion on formation of GaAs multiple concentric nanoring structures by droplet epitaxy," Chin. Phys. B **29**, 046801 (2020).
[71]Y. Y. Yan, M. H. Fang, X. B. Tang, F. D. Chen, H. Huang, X. Y. Sun, and L. L. Ji, "Effect of 150 keV proton irradiation on the performance of GaAs solar cells," Nucl. Instrum. Methods Phys. Res., Sect. B **451**, 49–54 (2019).
[72]T. Kanayama, "Recovery and accumulation of ion irradiation damage leading to dose rate dependence in GaAs," Jpn. J. Appl. Phys. **59**, 096504 (2020).
[73]L. B. B. Aji, J. B. Wallace, and S. O. Kucheyev, "Radiation defect dynamics in GaAs studied by pulsed ion beams," J. Appl. Phys. **124**, 025701 (2018).
[74]A. Debelle, G. Gutierrez, A. Boulle, I. Monnet, and L. Thomé, "Effect of energy deposition on the disordering kinetics in dual-ion beam irradiated single-crystalline GaAs," J. Appl. Phys. **132**, 085905 (2022).
[75]T. Mattila and R. M. Nieminen, "Direct antisite formation in electron-irradiation of GaAs," Phys. Rev. Lett. **74**, 2721–2724 (1995).
[76]M. Sayed, J. H. Jefferson, A. B. Walker, and A. G. Cullis, "Computer-simulation of atomic displacements in Si, GaAs, and AlAs," Nucl. Instrum. Methods Phys. Res., Sect. B **102**, 232–235 (1995).
[77]J. Nord, K. Nordlund, and J. Keinonen, "Amorphization mechanism and defect structures in ion-beam-amorphized Si, Ge, and GaAs," Phys. Rev. B **65**, 165329 (2002).
[78]C. Björkas, K. Nordlund, K. Arstila, J. Keinonen, V. D. S. Dhaka, and M. Pessa, "Damage production in GaAs and GaAsN induced by light and heavy ions," J. Appl. Phys. **100**, 053516 (2006).
[79]C. Björkas, K. Nordlund, K. Arstila, J. Keinonen, V. D. S. Dhaka, and M. Pessa, "Light and heavy ion effects on damage clustering in GaAs quantum wells," Nucl. Instrum. Methods Phys. Res., Sect. B **257**, 324–327 (2007).
[80]J. Mangeney, H. Choumane, G. Patriarche, G. Leroux, G. Aubin, J. C. Harmand, J. L. Oudar, and H. Bernas, "Comparison of light- and heavy-ion-irradiated quantum-wells for use as ultrafast saturable absorbers," Appl. Phys. Lett. **79**, 2722–2724 (2001).
[81]V. D. S. Dhaka, N. V. Tkachenko, H. Lemmetyinen, E. M. Pavelescu, M. Guina, A. Tukiainen, J. Konttinen, M. Pessa, K. Arstila, J. Keinonen, and K. Nordlund, "Effects of heavy-ion and light-ion irradiation on the room temperature carrier dynamics of InGaAs/GaAs quantum wells," Semicond. Sci. Technol. **21**, 661–664 (2006).
[82]F. Gao, N. J. Chen, E. Hernandez-Rivera, D. H. Huang, and P. D. Levan, "Displacement damage and predicted non-ionizing energy loss in GaAs," J. Appl. Phys. **121**, 095104 (2017).
[83]J. P. Biersack and J. F. Ziegler, "Refined universal potentials in atomic-collisions," Nucl. Instrum. Methods Phys. Res **194**, 93–100 (1982).
[84]J. L. Teunissen, T. Jarrin, N. Richard, N. E. Koval, D. M. Santiburcio, J. Kohanoff, E. Artacho, F. Cleri, and F. Da Pieve, "Effect of electronic stopping in molecular dynamics simulations of collision cascades in gallium arsenide," Phys. Rev. Mater. **7**, 025404 (2023).
[85]M. J. Norgett, M. T. Robinson, and I. M. Torrens, "Proposed method of calculating displacement dose-rates," Nucl. Eng. Des. **33**, 50–54 (1975).
[86]N. J. Chen, S. Gray, E. Hernandez-Rivera, D. H. Huang, P. D. Levan, and F. Gao, "Computational simulation of threshold displacement energies of GaAs," J. Mater. Res. **32**, 1555–1562 (2017).
[87]E. A. Burke, C. J. Dale, A. B. Campbell, G. P. Summers, W. J. Stapor, M. A. Xapsos, T. Palmer, and R. Zuleeg, "Energy-dependence of proton-induced displacement damage in gallium-arsenide," IEEE Trans. Nucl. Sci. **34**, 1220–1226 (1987).
[88]J. Lindhard, M. Scharff, and H. E. Schiott, Mat. Fys. Medd. Dan. Vidensk. Selsk. **33**, 1 (1963).
[89]S. R. Messenger, E. A. Burke, M. A. Xapsos, G. P. Summers, R. J. Walters, I. Jun, and T. Jordan, "NIEL for heavy ions: An analytical approach," IEEE Trans. Nucl. Sci. **50**, 1919–1923 (2003).
[90]W. R. Wampler and S. M. Myers, "Model for transport and reaction of defects and carriers within displacement cascades in gallium arsenide," J. Appl. Phys. **117**, 045707 (2015).
[91]P. A. Schultz and O. A. von Lilienfeld, "Simple intrinsic defects in gallium arsenide," Modell. Simul. Mater. Sci. Eng. **17**, 084007 (2009).
[92]G. D. Watkins, "Negative-U properties for defects in solids," Festkor-Adv. Solid State Phys. **24**, 163–189 (1984).

[93]J. Coutinho, V. P. Markevich, and A. R. Peaker, "Characterisation of negative-defects in semiconductors," J. Phys.: Condens. Matter **32**, 323001 (2020).
[94]H. P. Komsa and A. Pasquarello, "Assessing the accuracy of hybrid functionals in the determination of defect levels: Application to the As antisite in GaAs," Phys. Rev. B **84**, 075207 (2011).
[95]H. P. Komsa and A. Pasquarello, "Comparison of vacancy and antisite defects in GaAs and InGaAs through hybrid functionals," J. Phys.: Condens. Matter **24**, 045801 (2012).
[96]D. J. Chadi and K. J. Chang, "Metastability of the isolated arsenic-antisite defect in GaAs," Phys. Rev. Lett. **60**, 2187–2190 (1988).
[97]J. Dabrowski and M. Scheffler, "Isolated arsenic-antisite defect in GaAs and the properties of EL2," Phys. Rev. B **40**, 10391–10401 (1989).
[98]N. A. Modine, A. F. Wright, and S. R. Lee, "Bounds on the range of density-functional-theory point-defect levels in semiconductors and insulators," Comput. Mater. Sci. **92**, 431–438 (2014).
[99]E. R. Weber, H. Ennen, U. Kaufmann, J. Windscheif, J. Schneider, and T. Wosinski, "Identification of As_{Ga} antisites in plastically deformed GaAs," J. Appl. Phys. **53**, 6140–6143 (1982).
[100]J. Lagowski, D. G. Lin, T. P. Chen, M. Skowronski, and H. C. Gatos, "Native hole trap in bulk GaAs and its association with the double-charge state of the arsenic antisite defect," Appl. Phys. Lett. **47**, 929–931 (1985).
[101]P. Omling, P. Silverberg, and L. Samuelson, "Identification of a 2nd energy-level of EL2 in N-type GaAs," Phys. Rev. B **38**, 3606–3609 (1988).
[102]A. Bencherifa, G. Brémond, A. Nouailhat, G. Guillot, A. Guivarc'h, and A. Regreny, "On the identification of the double donor state of EL2 in P-type GaAs," Rev. Phys. Appl. **22**, 891–895 (1987).
[103]S. B. Zhang and D. J. Chadi, "Cation antisite defects and antisite-interstitial complexes in gallium-arsenide," Phys. Rev. Lett. **64**, 1789–1792 (1990).
[104]G. Bösker, N. A. Stolwijk, H. G. Hettwer, A. Rucki, W. Jäger, and U. Jäger, "Use of zinc diffusion into GaAs for determining properties of gallium interstitials," Phys. Rev. B **52**, 11927–11931 (1995).
[105]H. Bracht, M. S. Norseng, E. E. Haller, and K. Eberl, "Zinc diffusion enhanced Ga diffusion in GaAs isotope heterostructures," Physica B **308–310**, 831–834 (2001).
[106]H. Bracht and S. Brotzmann, "Zinc diffusion in gallium arsenide and the properties of gallium interstitials," Phys. Rev. B **71**, 115216 (2005).
[107]M. A. Malouin, F. El-Mellouhi, and N. Mousseau, "Gallium self-interstitial relaxation in GaAs: An *ab initio* characterization," Phys. Rev. B **76**, 045211 (2007).
[108]J. T. Schick and C. G. Morgan, "Gallium interstitial contributions to diffusion in gallium arsenide," AIP Adv. **1**, 032161 (2011).
[109]A. F. Wright and N. A. Modine, "Migration processes of the As interstitial in GaAs," J. Appl. Phys. **120**, 215705 (2016).
[110]D. Stievenard, X. Boddaert, and J. C. Bourgoin, "Irradiation-induced defects in P-type GaAs," Phys. Rev. B **34**, 4048–4058 (1986).
[111]J. C. Bourgoin and J. W. Corbett, "Enhanced diffusion mechanisms," Radiat. Eff. **36**, 157–188 (1978).
[112]C. E. Barnes, "Effects of Co_{60} gamma irradiation on epitaxial GaAs laser diodes," Phys. Rev. B **1**, 4735–4747 (1970).
[113]G. A. Baraff and M. Schluter, "Bistability and metastability of the gallium vacancy in GaAs—The actuator of EL2," Phys. Rev. Lett. **55**, 2340–2343 (1985).
[114]S. Pöykkö, M. J. Puska, M. Alatalo, and R. M. Nieminen, "Metastable defect complexes in GaAs," Phys. Rev. B **54**, 7909–7916 (1996).
[115]B. P. Uberuaga and R. Perriot, "Insights into dynamic processes of cations in pyrochlores and other complex oxides," Phys. Chem. Chem. Phys. **17**, 24215–24223 (2015).
[116]S. T. Murphy, B. P. Uberuaga, J. B. Ball, A. R. Cleave, K. E. Sickafus, R. Smith, and R. W. Grimes, "Cation diffusion in magnesium aluminate spinel," Solid State Ion. **180**, 1–8 (2009).
[117]B. P. Uberuaga and L. J. Vernon, "Interstitial and vacancy mediated transport mechanisms in perovskites: A comparison of chemistry and potentials," Solid State Ion. **253**, 18–26 (2013).
[118]G. A. Baraff and M. Schlüter, "Electronic-structure, total energies, and abundances of the elementary point-defects in GaAs," Phys. Rev. Lett. **55**, 1327–1330 (1985).
[119]F. El-Mellouhi and N. Mousseau, "Self-vacancies in gallium arsenide:: An *ab initio* calculation," Phys. Rev. B **71**, 125207 (2005).
[120]J. E. Northrup and S. B. Zhang, "Dopant and defect energetics—Si in GaAs," Phys. Rev. B **47**, 6791–6794 (1993).
[121]F. El-Mellouhi and N. Mousseau, "Charge-dependent migration pathways for the Ga vacancy in GaAs," Phys. Rev. B **74**, 205207 (2006).
[122]D. E. Bliss, W. Walukiewicz, and E. E. Haller, "Annealing of As-Ga-related defects in Lt-GaAs —the role of gallium vacancies," J. Electron. Mater. **22**, 1401–1404 (1993).
[123]G. A. Baraff and M. Schlüter, "Binding and formation energies of native defect pairs in GaAs," Phys. Rev. B **33**, 7346–7348 (1986).
[124]F. El-Mellouhi and N. Mousseau, "*Ab initio* characterization of arsenic vacancy diffusion pathways in GaAs with SIEST-A-RT," Appl. Phys. A **86**, 309–312 (2007).
[125]G. Zollo and R. M. Nieminen, "Small self-interstitial clusters in GaAs," J. Phys.: Condens. Matter **15**, 843–853 (2003).
[126]G. Zollo, Y. J. Lee, and R. M. Nieminen, "Properties of intrinsic di-interstitials in GaAs," J. Phys.: Condens. Matter **16**, 8991–9000 (2004).
[127]G. Zollo and F. Gala, "Stability of I3 complexes in III–V compound semiconductors by tight-binding molecular dynamics," Phys. Rev. B **75**, 115205 (2007).
[128]G. Zollo and F. Gala, "Properties of charged intrinsic di-interstitials in GaAs," Phys. Rev. B **77**, 094125 (2008).
[129]F. Gala and G. Zollo, "Nucleation and first-stage growth processes of extrinsic defects in GaAs triggered by self-interstitials," Phys. Rev. B **80**, 174113 (2009).
[130]G. Zollo and F. Gala, "Migration barriers of neutral As di-interstitials in GaAs," New J. Phys. **14**, 053036 (2012).
[131]M. Volpe, G. Zollo, and L. Colombo, "Structural, electronic, and energetic properties of small self-interstitial clusters in GaAs by tight-binding molecular dynamics," Phys. Rev. B **71**, 075207 (2005).
[132]P. A. Schultz, "The E1–E2 center in gallium arsenide is the divacancy," J. Phys.: Condens. Matter **27**, 075801 (2015).
[133]M. J. Puska and C. Corbel, "Positron states in Si and GaAs," Phys. Rev. B **38**, 9874–9880 (1988).
[134]T. E. M. Staab, M. Haugk, T. Frauenheim, and H. S. Leipner, "Magic number vacancy aggregates in GaAs: Structure and positron lifetime studies," Phys. Rev. Lett. **83**, 5519–5522 (1999).
[135]A. Barthel, L. Sayre, G. Kusch, R. A. Oliver, and L. C. Hirst, "Radiation effects in ultra-thin GaAs solar cells," J. Appl. Phys. **132**, 184501 (2022).
[136]B. K. Jones, J. Santana, and M. McPherson, "Semiconductor detectors for use in high radiation damage environments—semi-insulating GaAs or silicon?," Nucl. Instrum. Methods Phys. Res., Sect. A **395**, 81–87 (1997).
[137]E. H. Bogardus and H. B. Bebb, "Bound-exciton free-exciton band-acceptor donor-acceptor and Auger recombination in GaAs," Phys. Rev. **176**, 993 (1968).
[138]C. N. Singh, B. P. Uberuaga, S. J. Tobin, and X. Y. Liu, "Impact of radiation-induced point defects on thermal carrier decay processes in GaAs," Acta Mater. **242**, 118480 (2023).
[139]W. Shockley and W. T. Read, "Statistics of the recombinations of holes and electrons," Phys. Rev. **87**, 835–842 (1952).
[140]D. Steiauf, E. Kioupakis, and C. G. Van de Walle, "Auger recombination in GaAs from first principles," ACS Photonics **1**, 643–646 (2014).
[141]J. Shah and R. C. C. Leite, "Radiative recombination from photoexcited hot carriers in GaAs," Phys. Rev. Lett. **22**, 1304 (1969).
[142]G. W. 't Thooft, "The radiative recombination coefficient of GaAs from laser delay measurements and effective nonradiative carrier lifetimes," Appl. Phys. Lett. **39**, 389–390 (1981).
[143]A. Alkauskas, Q. M. Yan, and C. G. Van de Walle, "First-principles theory of nonradiative carrier capture via multiphonon emission," Phys. Rev. B **90**, 075202 (2014).
[144]A. M. Stoneham, "Nonradiative-transitions in semiconductors," Rep. Prog. Phys. **44**, 1251–1295 (1981).

[145]T. Wosinski, "Phonon-assisted tunnel emission of holes from the double donor level of the EL2 defect," Phys. Status Solidi B **253**, 1916–1922 (2016).
[146]H. Y. Chen, V. A. Jhalani, M. Palummo, and M. Bernardi, "Calculations of exciton radiative lifetimes in bulk crystals, nanostructures, and molecules," Phys. Rev. B **100**, 075135 (2019).
[147]S. A. Shahahmadi, P. Kivisaari, B. Behaghel, I. Radevici, S. Suihkonen, and J. Oksanen, "Pushing the limits of non-radiative recombination suppression in GaAs/GaInP light-emitting diodes by doping profile engineering," Appl. Phys. Lett. **124**, 241105 (2024).
[148]K. H. Zschauer, "Auger recombination in heavily doped P-type GaAs," Solid State Commun. **7**, 1709 (1969).
[149]G. Benz and R. Conradt, "Auger recombination in GaAs and GaSb," Phys. Rev. B **16**, 843–855 (1977).
[150]D. J. Robbins, "Auger recombination at the B-center in gallium-arsenide," J. Phys. C: Solid State Phys. **13**, L1073–L1078 (1980).
[151]U. Strauss, W. W. Rühle, and K. Köhler, "Auger recombination in intrinsic GaAs," Appl. Phys. Lett. **62**, 55–57 (1993).
[152]R. K. Ahrenkiel, R. Ellingson, W. Metzger, D. I. Lubyshev, and W. K. Liu, "Auger recombination in heavily carbon-doped GaAs," Appl. Phys. Lett. **78**, 1879–1881 (2001).
[153]M. Govoni, I. Marri, and S. Ossicini, "Auger recombination in Si and GaAs semiconductors: Results," Phys. Rev. B **84**, 075215 (2011).
[154]C. N. Singh, X. Y. Liu, B. P. Uberuaga, and S. J. Tobin, "Reduction of bright exciton lifetimes by radiation-induced disorder," Phys. Rev. Mater. **5**, 073802 (2021).
[155]D. H. Kim, J. H. Lee, and S. K. Son, "Band-structure simulations for overlap wave functions between electrons and holes for recombination in undoped GaAs/AlGaAs heterostructures," J. Korean Phys. Soc. **80**, 161–166 (2022).
[156]G. Pirard, F. B. Basset, S. Bietti, S. Sanguinetti, R. Trotta, and G. Bester, "Effects of random alloy disorder, shape deformation, and substrate misorientation on the exciton lifetime and fine structure splitting of GaAs/$Al_xGa_{1-x}As$ (111) quantum dots," Phys. Rev. B **107**, 205417 (2023).
[157]K. Leosson, J. R. Jensen, W. Langbein, and J. M. Hvam, "Exciton localization and interface roughness in growth-interrupted GaAs/AlAs quantum wells," Phys. Rev. B **61**, 10322–10329 (2000).
[158]A. Maros, N. N. Faleev, M. I. Bertoni, C. B. Honsberg, and R. R. King, "Carrier localization effects in GaAsSb/GaAs heterostructures," J. Appl. Phys. **120**, 183104 (2016).
[159]M. Jansson, V. V. Nosenko, G. Y. Rudko, F. Ishikawa, W. M. Chen, and I. A. Buyanova, "Lattice dynamics and carrier recombination in GaAs/GaAsBi nanowires," Sci. Rep. **13**, 12880 (2023).
[160]M. Oliva, T. Flissikowski, M. Góra, J. Lähnemann, J. Herranz, R. B. Lewis, O. Marquardt, M. Ramsteiner, L. Geelhaar, and O. Brandt, "Carrier recombination in highly uniform and phase-pure GaAs/(Al,Ga)As core/shell nanowire arrays on Si(111) implications for light-emitting devices," ACS Appl. Nano Mater. **6**, 15278–15293 (2023).
[161]J. Heyd, G. E. Scuseria, and M. Ernzerhof, "Hybrid functionals based on a screened Coulomb potential," J. Chem. Phys. **118**, 8207–8215 (2003).
[162]J. P. Perdew, M. Ernzerhof, and K. Burke, "Rationale for mixing exact exchange with density functional approximations," J. Chem. Phys. **105**, 9982–9985 (1996).
[163]T. Jourdan, G. Bencteux, and G. Adjanor, "Efficient simulation of kinetics of radiation induced defects: A cluster dynamics approach," J. Nucl. Mater. **444**, 298–313 (2014).
[164]A. A. Kohnert, B. D. Wirth, and L. Capolungo, "Modeling microstructural evolution in irradiated materials with cluster dynamics methods: A review," Comput. Mater. Sci. **149**, 442–459 (2018).
[165]J. Marian and V. V. Bulatov, "Stochastic cluster dynamics method for simulations of multispecies irradiation damage accumulation," J. Nucl. Mater. **415**, 84–95 (2011).
[166]A. A. Kohnert and B. D. Wirth, "Grouping techniques for large-scale cluster dynamics simulations of reaction diffusion processes," Modell. Simul. Mater. Sci. Eng. **25**, 015008 (2017).
[167]C. Matthews, R. Perriot, M. W. D. Cooper, C. R. Stanek, and D. A. Andersson, "Cluster dynamics simulation of xenon diffusion during irradiation in UO_2," J. Nucl. Mater. **540**, 152326 (2020).
[168]C. Matthews, R. Perriot, M. W. D. Cooper, C. R. Stanek, and D. A. Andersson, "Cluster dynamics simulation of uranium self-diffusion during irradiation in UO," J. Nucl. Mater. **527**, 151787 (2019).
[169]D. H. Huang, A. Iurov, F. Gao, G. Gumbs, and D. A. Cardimona, "Many-body theory of proton-generated point defects for losses of electron energy and photons in quantum wells," Phys. Rev. Appl. **9**, 024002 (2018).
[170]L. A. Marqués, L. Pelaz, J. Hernández, J. Barbolla, and G. H. Gilmer, "Stability of defects in crystalline silicon and their role in amorphization," Phys. Rev. B **64**, 045214 (2001).
[171]L. A. M. Rosset, D. A. Drabold, and V. L. Deringer, "Signatures of paracrystallinity in amorphous silicon from machine-learning-driven molecular dynamics," Nat. Commun. **16**, 2360 (2025).
[172]I. Jenčič, M. W. Bench, I. M. Robertson, and M. A. Kirk, "Electron-Beam-Induced crystallization of isolated amorphous regions in Si, Ge, GaP, and GaAs," J. Appl. Phys. **78**, 974–982 (1995).
[173]A. Leiberich, D. M. Maher, R. V. Knoell, and W. L. Brown, "Ion-beam induced crystallization and amorphization at a crystalline amorphous interface in [100] silicon," Nucl. Instrum. Methods Phys. Res., Sect. B **19–20**, 457–461 (1987).
[174]L. A. Marqués, L. Pelaz, P. López, I. Santos, and M. Aboy, "Recrystallization of atomically balanced amorphous pockets in Si: A source of point defects," Phys. Rev. B **76**, 153201 (2007).
[175]S. S. Navale and M. J. Demkowicz, "Vacancy and interstitial interactions with crystal/amorphous, metal/covalent interfaces," J. Nucl. Mater. **539**, 152329 (2020).
[176]K. R. C. Mok, M. Jaraiz, I. Martin-Bragado, J. E. Rubio, P. Castrillo, R. Pinacho, J. Barbolla, and M. P. Srinivasan, "Ion-beam amorphization of semiconductors: A physical model based on the amorphous pocket population," J. Appl. Phys. **98**, 046104 (2005).
[177]M. J. Zheng, N. Swaminathan, D. Morgan, and I. Szlufarska, "Energy barriers for point-defect reactions in 3-SiC," Phys. Rev. B **88**, 054105 (2013).
[178]P. Żukowski, T. Koltunowicz, J. Partyka, P. Węgierek, F. F. Komarov, A. M. Mironov, N. Butkievith, and D. Freik, "Dielectric properties and model of hopping conductivity of GaAs irradiated by H ions," Vacuum **81**, 1137–1140 (2007).
[179]N. Papež, A. Gajdoš, D. Sobola, R. Dallaev, R. Macků, P. Škarvada, and L. Grmela, "Effect of gamma radiation on properties and performance of GaAs based solar cells," Appl. Surf. Sci. **527**, 146766 (2020).
[180]J. Guo, B. K. Chang, M. Z. Yang, H. G. Wang, and M. S. Wang, "The study of the optical properties of the GaAs with point defects," Optik **125**, 419–423 (2014).
[181]H. J. Queisser, H. C. Casey, and W. van Roosbroeck, "Carrier transport and potential distributions for a semiconductor p-n junction in the relaxation regime," Phys. Rev. Lett. **26**, 551–554 (1971).
[182]M. C. Wu, Y. H. Huang, and C. L. Ho, "High-speed InGaP/GaAs p–i–n photodiodes with wide spectral range," IEEE Electron Device Lett. **28**, 797–799 (2007).
[183]N. Pap, R. Dallaev, S. Talu, and J. Kagtyl, "Overview of the current state of gallium arsenide-based solar cells," Materials **14**, 3075 (2021).
[184]A. Phakkhawan, A. Sakulkalavek, S. Buranurak, P. Klangtakai, K. Pangza, N. Jangsawang, S. Nasompag, M. Horprathum, S. Kijamnajsuk, and S. Sanorpim, "Investigation of radiation effect on structural and optical properties of GaAs under high-energy electron irradiation," Materials **15**, 5897 (2022).
[185]M. G. Craford, "LEDs challenge the incandescents," IEEE Circuits Devices Mag. **8**, 24–29 (1992).
[186]K. C. Dimiduk, C. Q. Ness, and J. K. Foley, "Electron-irradiation of GaAsP LEDs," IEEE Trans. Nucl. Sci. **32**, 4010–4015 (1985).
[187]R. Vernydub, O. Kyrylenko, O. Konoreva, O. Radkevych, D. Stratilat, and V. Tartachnyk, "Radiation defects in GaP, GaAsP, InGaN LEDs"; R. Vernydub, O. Kyrylenko, O. Konoreva, O. Radkevych, D. Stratilat, and V. Tartachnyk,

"Radiation defects in GaP, GaAsP, InGaN LEDs" RAD Conf. Proc. **5**, 84–89 (2021).
[188]S. L. Yellen, A. H. Shepard, R. J. Dalby, J. A. Baumann, H. B. Serreze, T. S. Guido, R. Soltz, K. J. Bystrom, C. M. Harding, and R. G. Waters, "Reliability of GaAs-based semiconductor diode-lasers—0.6-1.1-mu-m," IEEE J. Quantum Electron. **29**, 2058–2067 (1993).
[189]H. Lischka, P. Clemens, H. Henschel, O. Kohn, W. Lennartz, and H. U. Schmidt, "Radiation effects in optoelectronic devices," in Proceedings of the Society of Photo-Optical Instrumentation (1994), Vol. 2425, pp. 43–52.
[190]J. Kaniewski and J. Piotrowski, "InGaAs for infrared photodetectors. Physics and technology," Opto-Electron Rev. **12**, 139–148 (2004).
[191]S. J. Xu, S. J. Chua, T. Mei, X. C. Wang, X. H. Zhang, G. Karunasiri, W. J. Fan, C. H. Wang, J. Jiang, S. Wang, and X. G. Xie, "Characteristics of InGaAs quantum dot infrared photodetectors," Appl. Phys. Lett. **73**, 3153–3155 (1998).
[192]H. B. Jo, D. Y. Yun, J. M. Baek, J. H. Lee, T. W. Kim, D. H. Kim, T. Tsutsumi, H. Sugiyama, and H. Matsuzaki, "L_g = 25 nm InGaAs/InAlAs high-electron mobility transistors with both and in excess of 700 GHz," Appl. Phys. Express **12**, 054006 (2019).
[193]R. S. Geels, S. W. Corzine, and L. A. Coldren, "InGaAs vertical-cavity surface-emitting lasers," IEEE J. Quantum Electron. **27**, 1359–1367 (1991).
[194]S. Kawakita, M. Imaizumi, K. Makita, J. Nishinaga, T. Sugaya, H. Shibata, S. I. Sato, and T. Ohshima, "High efficiency and radiation resistant InGaP/GaAs//CIGS stacked solar cells for space applications," in *IEEE Photovoltaics Specialists Conference* (IEEE, 2016), pp. 2574–2577.
[195]L. Olantera, F. Bottom, A. Kraxner, S. Detraz, M. Menouni, P. Moreira, C. Scarcella, C. Sigaud, C. Soos, J. Troska, and F. Vasey, "Radiation effects on high-speed InGaAs photodiodes," IEEE Trans. Nucl. Sci. **66**, 1663–1670 (2019).
[196]T. S. Kim, H. J. Kim, D. M. Geum, J. H. Han, I. S. Kim, N. Hong, G. H. Ryu, J. Kang, W. J. Choi, and K. J. Yu, "Ultra-lightweight, flexible InGaP/GaAs tandem solar cells with a dual-function encapsulation layer," ACS Appl. Mater. Interfaces **13**, 13248–13253 (2021).
[197]T. Takamoto, E. Ikeda, H. Kurita, and M. Ohmori, "Over 30% efficient InGaP/GaAs tandem solar cells," Appl. Phys. Lett. **70**, 381–383 (1997).
[198]V. Donchev, M. Milanova, and S. Georgiev, "Surface photovoltage study of GaAsSbN and GaAsSb layers grown by LPE for solar cells applications," Energies **15**, 6563 (2022).
[199]G. Stillman, L. Cook, N. Tabatabaie, G. Bulman, and V. Robbins, "InGaAsP photodiodes," IEEE Trans. Electron Devices **30**, 364–381 (1983).
[200]T. Sugaya, Y. Nagato, Y. Okano, R. Oshima, T. Tayagaki, K. Makita, and K. Matsubara, "Growth of InGaAsP solar cells and their application to triple-junction top cells used in smart stack multijunction solar cells," J. Vac. Sci. Technol. B **35**, 02B103 (2017).
[201]Y. Kashima, A. Matoba, and H. Takano, "Linear InGaAsP edge-emitting LEDs for single-mode fiber communications," J. Lightwave Technol. **10**, 1650–1655 (1992).
[202]T. Pearsall, "Indium gallium arsenide phosphide," in *Encyclopedia of Materials: Science and Technology*, edited by K. H. J. Buschow, R. W. Cahn, M. C. Flemings, B. Ilschner, E. J. Kramer, S. Mahajan, and P. Veyssière (Elsevier, 2001), pp. 4048–4061.
[203]H. Ohyama, E. Simoen, C. Claeys, T. Hakata, T. Kudou, M. Yoneoka, K. Kobayashi, M. Nakabayashi, Y. Takami, and H. Sunaga, "Radiation-induced lattice defects in InGaAsP laser diodes and their effects on device performance," Physica B **273–274**, 1031–1033 (1999).
[204]F. D. Chen, M. J. Zong, Z. X. Tan, and X. B. Tang, "Degradation characteristics and equivalent analysis of InGaAsP space solar cells under proton and neutron irradiation," Microelectron. Reliab. **151**, 115249 (2023).
[205]S. F. Ren, M. A. Bhuiyan, J. Y. Zhang, X. B. Lou, M. W. Si, X. Gong, R. Jiang, K. Ni, X. Wan, E. X. Zhang, R. G. Gordon, R. A. Reed, D. M. Fleetwood, P. D. Ye, and T. P. Ma, "Total ionizing dose (TID) effects in GaAs MOSFETs with La-based epitaxial gate dielectrics," IEEE Trans. Nucl. Sci. **64**, 164–169 (2017).
[206]O. A. Plaksin and V. A. Stepanov, "Radiation-induced electrical and optical processes in materials based on Al_2O_3," Opt. Spectrosc. **90**, 542–551 (2001).